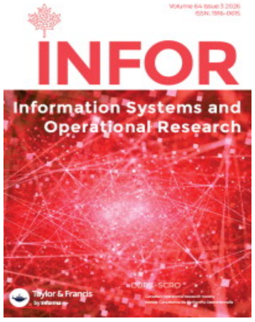

INFOR: Information Systems and Operational Research

ISSN: 0315-5986 (Print) 1916-0615 (Online) Journal homepage: www.tandfonline.com/journals/tinf20

Coordinating environmental policy and transmission planning in decentralised electricity industries

Afzal S. Siddiqui, Makoto Tanaka & Yihsu Chen

INFOR: INFORMATION SYSTEMS AND OPERATIONAL RESEARCH
https://doi.org/10.1080/03155986.2026.2629182

Coordinating environmental policy and transmission planning in decentralised electricity industries

Afzal S. Siddiqui[a,b], Makoto Tanaka[c] and Yihsu Chen[d]

[a]Department of Computer and Systems Sciences, Stockholm University, Kista, Sweden; [b]Department of Mathematics and Systems Analysis, Aalto University, Aalto, Finland; [c]National Graduate Institute for Policy Studies (GRIPS), Tokyo, Japan; [d]Department of Electrical and Computer Engineering, University of California at Santa Cruz, Santa Cruz, CA, USA

ABSTRACT

We use a bi-level framework to address how transmission planning may adapt to the cost of damage from emissions and imperfect competition in both greenfield and brownfield settings. Our upper level comprises a welfare-maximising transmission planner who internalises the damage cost in anticipation of generation operations at the lower level by profit-maximising firms. In a greenfield setting, i.e. without any existing capacity, complete CO_2 taxation on firms is optimal under perfect competition, and the CO_2 tax monotonically increases transmission capacity. By contrast, Cournot behaviour by industry chokes off consumption, thereby limiting the damage from CO_2 emissions and rendering partial CO_2 taxation optimal. In a brownfield Western European setting with perfect competition, only complete internalisation of the cost of damage from emissions provides the price signal to reduce consumption and to spur generation investment as in the greenfield setting. However, the brownfield setting with Cournot behaviour leads to fossil-fuel expansion by price-taking fringe firms, which exacerbates damage from CO_2 emissions vis-à-vis the greenfield setting. Hence, it is optimal to fully internalise the cost of damage from emissions with complementary expansion of the transmission network in a brownfield setting even with market power in contrast to the result in a greenfield setting.

ARTICLE HISTORY
Received 26 November 2024
Accepted 4 February 2026

KEYWORDS
Or in energy; transmission planning; market power; carbon policy

1. Introduction

Largely constructed in the post-World War II era, high-voltage transmission networks in most OECD countries' electricity industries were designed to harness the economies of scale of large fossil-fuelled and nuclear power plants. Under vertical integration, a cost-minimisation framework (Garver 1970) could underpin an integrated

CONTACT Afzal S. Siddiqui asiddiq@dsv.su.se Department of Computer and Systems Sciences, Stockholm University, P.O. Box 1073, 164 25 Kista, Sweden.

Supplemental data for this article can be accessed online at https://doi.org/10.1080/03155986.2026.2629182.

resource plan to support investment decisions in both generation and transmission capacity. However, such an approach was outmoded by the 1990s due to increased efficiencies of small-scale generators (Hobbs 1995) and deregulation of the power sector (Wilson 2002). In particular, deregulation introduced competition in generation by unbundling it from transmission and distribution services. Thus, a current challenge for transmission planning is to anticipate the addition of generation capacity by profit-maximising power companies that often have objectives in conflict with welfare maximisation.

More recently, environmental concerns have necessitated further transformation of the power sector. Instead of relying upon centralised, controllable power plants, the so-called Green New Deal envisages decarbonisation of the power sector and electrification of other energy sectors.[1] The concomitant investment in variable renewable energy (VRE), viz., wind and solar power, means that generation sources will become largely dispersed and intermittent. Hence, the transmission network will have to adapt to a vastly different paradigm in order to balance potentially conflicting economic and environmental objectives (Lau and Hobbs 2021).

Together, the twin trends of deregulation and decarbonisation pose a quandary for policymakers. In effect, they have simultaneously committed to higher environmental standards for the power sector while having relinquished direct control over it. Moreover, while climate treaties imply legally binding targets, policymakers cannot be seen to be interfering with industry. Consequently, they must strike a delicate balance between providing incentives to guide a sustainable energy transition and blunting the market's ability to function. Specifically, policymakers should anticipate the economic and environmental consequences of generation capacity adopted by power companies when proposing transmission-investment plans and setting carbon prices.

Work on transmission planning has duly focused on integrating VRE in a deregulated power sector. Motivated by uncertainty that stems from VRE output and demand, recent efforts on transmission planning have taken into account the value of flexibility over technology choice *via* real options (Mariscal et al. 2020) and assessed the performance of robust optimisation vis-à-vis that of stochastic programming (Mahmoud et al. 2024; Rintamäki et al. 2024). The framework for robust optimisation has also been enhanced to address issues related to high VRE penetration (Yin et al. 2023; Zeng et al. 2024). Yet, such perspectives typically assume either a cost-minimising or welfare-maximising social planner without explicitly accounting for either environmental externalities (Sun et al. 2025) or imperfect competition. The latter aspect is well studied in terms of market power among generators (Skoulidas et al. 2010; Gabriel et al. 2013), and recent advances in solution methods for leader-follower games (Cambini and Riccardi 2024; García-Cerezo et al. 2025) are couched similarly. However, as Chen et al. (2020) and Tanaka et al. (2022) point out, the overlap between economic and environmental distortions is especially pertinent for transmission planning and necessitates careful treatment.

In this vein, Baringo and Conejo (2012)'s bi-level model considers cost-minimising wind and transmission investment at the upper level constrained by lower-level market operations that are marked by uncertainty, e.g. in demand and wind output. Although the paper's focus is a methodological one in implementing computationally tractable problem instances of a stochastic mathematical program with equilibrium constraints (MPEC) for realistic test networks, it also provides policy insights concerning the role of subsidies in spurring wind investment. Specifically, it is shown that a moderate subsidy, e.g. 20% of the investment cost, can nearly double the adopted wind capacity. Also using a bi-level framework, Maurovich-Horvat et al. (2015) address market power by power companies, which decide upon generation investment and operations at the lower level. Meanwhile, the upper level could comprise either a welfare-maximising transmission system operator (TSO) or a profit-maximising merchant investor (MI) that determines transmission investment in anticipation of market outcomes. Their main finding is that an MI typically invests in less capacity than the TSO does in order to maintain high nodal price differences. Furthermore, regardless of whether the transmission planner is an MI or a TSO, Cournot behaviour by firms leads to more wind investment. In effect, withholding of capacity by firms induces the TSO to increase welfare by implicitly subsidising wind, whereas the MI accommodates more power flow to boost profit.

While such bi-level models for transmission planning incorporate VRE adoption, they tend to focus on proxy measures to gauge the environmental impact. For example, Maurovich-Horvat et al. (2015) consider the proportion of energy generated from wind, which is related to renewable portfolio standards (RPS). While RPS is straightforward to grasp as a policy target, e.g. 50% of energy should be based on renewables, Hobbs (2012) cautions against relying on such proxy measures to guide the sustainable energy transition. This is because proxy measures may not accurately reflect the tradeoff between the underlying metrics, viz., welfare and emissions, as part of an investment plan. Thus, a capacity-adoption outcome with a high share of VRE output may appear superficially attractive, but it may be detrimental to welfare because it actually comprises ‘too much’ renewable energy. Instead, the literature on environmental economics directly addresses the tradeoff between welfare and emissions by inserting a so-called damage cost in the regulator’s objective function (Barnett 1980; Requate 2006). By doing so, it is possible for the regulator to assess transparently the tradeoff between welfare and emissions. Specifically, a low damage cost may prioritise curbing of emissions *via* reduced consumption instead of expanded VRE investment. Only for a sufficiently high damage cost is it worthwhile to adopt renewables. Furthermore, the regulator can anticipate imperfect competition at the lower level and adapt to it, e.g. by reducing the carbon tax vis-à-vis perfect competition to offset the chokehold on consumption from market power.

Using a stylised two-node bi-level model, Siddiqui et al. (2019) take this environmental-economics approach to assess economic and environmental tradeoffs. At the upper level, they have a welfare-maximising TSO that internalises the cost of damage from emissions. They allow for strategic behaviour (Cournot oligopoly) or not (perfect competition) at the lower level by producers in order to compare different market settings: central planning (CP), perfect competition (PC), and Cournot oligopoly (CO). This setup enables an assessment of the impact of the cost of damage from emissions on the transmission plan either with or without a carbon tax. In particular, they find that transmission investment is curtailed under PC without a carbon tax vis-à-vis CP. This is because the node with the cheap (but polluting) thermal plant does not receive the price signal to curb consumption and is still incentivised to export power to the node with the expensive (but clean) renewable plant. In order to mitigate the environmental consequences, the TSO reduces the transmission capacity. A full carbon tax (Arora et al. 2018) on industry under PC results in a first-best solution by curbing consumption. By contrast, a full carbon tax under CO may actually worsen welfare vis-à-vis no tax because it further reduces consumer surplus. As a countervailing measure, the TSO increases the size of the line to allow more generation from the renewable plant to be exported. Yet, this outcome is inefficient because it requires 'too much' renewable energy and complementary transmission capacity. Instead, a second-best solution would be to impose a partial carbon tax.

In the literature on bi-level transmission planning, the focus has been on either computational implementation of large-scale problem instances without consideration of the damage cost or stylised models that attempt to internalise the damage cost. Thus, the extent to which the carbon price and transmission plan interact to mitigate the cost of damage from CO_2 emissions in imperfectly competitive power sectors has not been studied in realistic test networks. While some recent efforts address this divide, their emphasis is on either delineating the distinction between straightforward withholding and temporal arbitrage (Hassanzadeh Moghimi et al. 2024) or assessing the role of support measures without explicitly tackling externalities and market power (Belyak et al. 2024). In effect, an assessment of economic and environmental distortions in a generalisable power system with transmission expansion has been lacking.

Given this research gap, we aim to gain insights about the impacts of environmental policy and transmission planning in power systems by tackling the following research questions (RQs):

RQ 1. *How is transmission planning affected by internalising the cost of damage from CO_2 emissions?*

RQ 2. *How much of the cost of damage from CO_2 emissions should be internalised as a carbon tax under imperfect competition?*

We use both an illustrative greenfield example, i.e. without existing generation and transmission capacity, and a brownfield case study, which is based on 2017 Western European data (Virasjoki et al. 2020). In the illustrative example, we answer RQ 1 by noting that the absence of a carbon tax under PC does not provide a price signal for sufficient VRE investment. Consequently, the power system remains reliant on fossil-fuelled capacity, and the TSO proactively mitigates this inefficiency by reducing transmission capacity as the damage cost increases *ceteris paribus* to prevent the export of fossil-fuelled power. A carbon tax that fully reflects the cost of damage from emissions is socially optimal in that it curbs consumption sufficiently to eradicate the dirtiest fossil-fuelled capacity and to replace it largely with VRE. There is a corresponding increase in transmission capacity vis-à-vis PC without a carbon tax to enable VRE to meet demand throughout the network. As for RQ 2, we find that social welfare does not always monotonically increase in the carbon tax under CO. This is because the exercise of market power chokes off consumption and creates another distortion in addition to emissions. Thus, the further loss in consumer surplus from a higher carbon tax more than offsets the mitigation of emissions, and a partial carbon tax is preferable (Siddiqui et al. 2019). In contrast to extant illustrative studies on bi-level transmission planning, e.g. Baringo and Conejo (2012) and Maurovich-Horvat et al. (2015), the role of partial CO_2 pricing is explicitly tackled.

For the case study, the answer to RQ 1 under PC is similar, i.e. a higher carbon tax monotonically improves social welfare and alters the transmission plan to integrate VRE. However, it does not necessarily result in more transmission capacity; instead, the network topology with a full carbon tax is reconfigured to balance new intermittent VRE output with both flexible generation resources and reduced consumption. By contrast, the optimal transmission plan under PC without a carbon tax attempts to juggle solely existing generation resources to mitigate the cost of damage from emissions. The impact of market power in RQ 2 for the case study is actually quite different from that in the illustrative example due to the presence of fringe firms. Once firms with market power withhold generation under CO, fringe firms invest in new capacity, thereby tempering concern about market power in contrast to the illustrative example. Absent a carbon tax, fringe firms under CO invariably adopt combined-cycle gas turbine (CCGT) capacity instead of VRE, which makes environmental damage more pernicious in the case study. Unlike related work on regional case studies, e.g. Belyak et al. (2024) and Hassanzadeh Moghimi et al. (2024), we distil how insights may be affected by greenfield and brownfield assumptions. Hence, a carbon tax monotonically increases welfare and induces the TSO to invest in more lines as the internalisation of the damage cost incentivises firms to invest in the 'right' technology, i.e. VRE, instead of CCGT.

The rest of this paper is organised as follows. Section 2 outlines the assumptions used in the centralised and bi-level approaches. The central-planning and bi-level formulations are in Section 3 along with necessary reformulations. Section 4 implements numerical examples to investigate RQs 1–2. Section 5 summarises the work's findings, discusses its policy implications, and outlines directions for future research. Supplementary Appendices A, B, C, and D contain the nomenclature, the components for the reformulation of the bi-level model, supplementary results, and calculation of social welfare, respectively.

2. Research methodology

Our framework for analysis is a bi-level model (Gabriel et al. 2013) in which a welfare-maximising TSO selects transmission capacity at the upper level. Meanwhile, given the transmission capacities, the lower level is a Nash-Cournot game over a network (Hashimoto 1985; Hobbs 2001). In particular, we have a transmission network that comprises $n \in \mathcal{N}$ nodes each with inverse-demand function $A_{m,n,t} - Z_{m,n,t}c_{m,n,t}$, where $c_{m,n,t}$ (in MWh) is consumption at node n in period $t \in \mathcal{T}$ of week $m \in \mathcal{M}$. Here, $A_{m,n,t}$ (in €/MWh) and $Z_{m,n,t}$ (in €/MWh^2) are finite, positive parameters reflecting the intercept and slope, respectively, for inverse demand, which may vary by period and week. These inverse-demand functions passively represent consumers in our model. We weight representative weeks by W_m and have several periods in each week to capture variability in both demand and VRE availability. Each period has length T_t (in h). In order to handle boundary conditions with pumped-hydro storage (PHS) and power plants' ramping, we denote $\mathcal{T}^{\text{ini}}$ and $\mathcal{T}^{\text{fin}}$ as the subsets of time periods that exclude the first and the last, respectively, time period of the set $\mathcal{T}$. Connecting the nodes of the power system are $\ell \in \mathcal{L}$ transmission lines. Investment decisions regarding transmission capacity, $x_{j,\ell} \in \{0,1\}$, are made by a welfare-maximising TSO at the upper level and cannot be adapted to each weekly period. In other words, the TSO cannot directly make lower-level decisions but can implicitly account for the impact of its transmission investment on industry equilibria *via* the lower-level decisions, Ω^{LL}, and dual variables, Ω^{DV}. The binary transmission-investment decision, $x_{j,\ell}$, selects a discrete capacity level $j \in \mathcal{J}_\ell$ for each line ℓ that corresponds to a capacity size, $K^{\mathrm{trn}}_{j,\ell}$ (in MW), susceptance, $B_{j,\ell}$ (in S, which stands for 'siemens'), and amortised cost, $C^{\mathrm{trn}}_{j,\ell}$ (in €).

By contrast, generation investment, $z_{i,n,u}$ (in MW), is continuous for a unit $u \in \mathcal{U}_{i,n}$ that is located at node n and belongs to firm $i \in \mathcal{I}$. Associated with $z_{i,n,u}$ are amortised capacity costs, $C^{\mathrm{gen}}_{i,n,u}$ (in €/MW), and these decisions are made by profit-maximising firms $i \in \mathcal{I}$ at the lower level. At the same level, each firm decides how much installed capacity to make available for operations, $a_{i,n,u}$ (in MW), with associated amortised fixed operating and maintenance (O&M) costs, $C^{\mathrm{ava}}_{i,n,u}$ (in €/MW). [2] We take an open-loop approach in which generation-investment and capacity-availability decisions at the lower level are treated as if they were made at the same time as the operational ones, but the latter are adapted to each periodic condition (Maurovich-Horvat et al. 2015).

Each firm i owns a portfolio of power plants $u \in \mathcal{U}_{i,n}$ located at node n with output for plants limited by installed capacity, $K^{\mathrm{gen}}_{i,n,u}$ (in MW), plus capacity additions, $z_{i,n,u}$ (in MW). In terms of operational decisions, each plant $u \in \mathcal{U}_{i,n}$ produces $y_{i,m,n,t,u}$ (in MWh) in week m and period t. For VRE plants, the output is subject to minimum and maximum period-specific availability factors, $\underline{G}_{m,n,t,u}$ and $\overline{G}_{m,n,t,u}$, respectively. Up- and down-ramping rates of plants are modelled by R^{up}_u and R^{down}_u, respectively. $\underline{G}_{m,n,t,u}$, $\overline{G}_{m,n,t,u}$, R^{up}_u, and R^{down}_u are unitless parameters between 0 and 1. Following Virasjoki et al. (2020), we impose boundary conditions to deactivate plants' ramping constraints in the initial period of each week in order to avoid infeasibilities. Associated with fossil-fuelled output are operating costs, C^{opr}_u (in €/MWh), and CO_2 emission rates, F_u (in t/MWh, where 't' is 'tonne').[3] These rates are used to calculate total system emissions, $\sum_{i\in\mathcal{I}}\sum_{m\in\mathcal{M}}\sum_{n\in\mathcal{N}}\sum_{t\in\mathcal{T}}\sum_{u\in\mathcal{U}_{i,n}} W_m F_u y_{i,m,n,t,u}$. The cost of damage from emissions is included in social welfare (Labriet and Loulou 2003) as a linear function of the parameter D (in €/t).[4] However, the private cost to firms from CO_2 emissions depends on the parameter $H \in [0,1]$ that captures the fraction of the social cost of damage from CO_2 emissions that is passed on to industry as a carbon tax. For example, if total CO_2 emissions are 10 t and D equals €100/t, then the social cost of damage from CO_2 emissions is €1000, but the private cost is only €$H \times 1000$.

Power flows use a lossless DC load-flow approach based on susceptances, $B_{j,\ell}$, and voltage angles, $v_{m,n,t}$ (in rad). Specifically, the power flow in capacity level $j \in \mathcal{J}_\ell$ for each line ℓ in week m and period t is $f_{j,\ell,m,t}$ (in MW), which depends on the voltage-angle difference between nodes connected by line ℓ and the susceptance level. These are added over all $j \in \mathcal{J}_\ell$ for each line ℓ to determine the realised power flow, $\hat{f}_{\ell,m,t}$ (in MW). Power flows are decided by a surplus-maximising independent system operator (ISO) (Sauma and Oren 2006). Finally, Kirchhoff's laws require energy balance at each node and in every period.

PHS is modelled by keeping track of the storage level, $r^{\mathrm{sto}}_{i,m,n,t}$ (in MWh), at the end of period t in week m at node n belonging to firm i. The storage capacity belonging to firm i at node n is $\overline{R}_{i,n}$ (in MWh). The minimum storage capacity is controlled by $\underline{R}_{i,n}$, which is a unitless parameter between 0 and 1. We assume that each PHS unit's stored energy is at the minimum level at the beginning of each week. Any excess energy stored in PHS above the minimum level at the end of the week cannot be carried forward to the next week. While this conservative treatment of PHS operations understates storage's flexibility, leaving out inter-seasonal constraints is justified because we focus on transmission and not PHS. Decision variables that change the storage level are charging and discharging during period t in week m at node n by firm i, $r^{\text{in}}_{i,m,n,t}$ (in MWh) and $r^{\text{out}}_{i,m,n,t}$ (in MWh), respectively. The maximum rate at which PHS may be charged or discharged is $R^{\text{in}}_{i,n}$ (in MW/MWh) or $R^{\text{out}}_{i,n}$ (in MW/MWh), respectively.[5] Finally, the periodic storage efficiency and charging efficiency are E^{sto} and E^{in}, respectively, which are both unitless parameters in $[0,1]$.

In a deregulated industry, each firm maximises its own profit at the lower level by selecting generation investment, available capacity, generation output, and storage decisions while taking as given (i) the transmission capacity set by the TSO at the upper level, (ii) the decisions of all other firms at the lower level, and (iii) the decisions of the ISO at the lower level, i.e. the Nash supposition. Each firm acts as either a price taker under PC or a Cournot oligopolist. The ISO at the lower level manages net imports to maximise gross consumer surplus and takes the transmission capacity as given along with the firms' decisions. It is expedient to express the lower-level equilibrium problem as a single-agent quadratic program (QP). We subsequently resolve the bi-level problem by replacing the lower-level QP by its primal constraints, dual constraints, and the strong-duality expression (SDE). Consequently, the resulting mathematical program with primal and dual constraints (MPPDC) is reformulated as a mixed-integer quadratically constrained quadratic program (MIQCQP) after linearising the lower level's primal and dual constraints (Virasjoki et al. 2020).

3. Problem formulation

In Section 3.1, we provide a benchmark CP formulation in which a single welfare-maximising entity makes all decisions. The bi-level formulation is then provided in Section 3.2 with subsequent MPPDC and MIQCQP reformulations in Sections 3.3 and 3.4, respectively.

3.1. Central planning

In a first-best benchmark, a central planner maximises social welfare (SW) including the cost of damage from emissions (1a):

$$
\begin{aligned}
\underset{\Omega^{\text{CP}}}{\text{Maximise}} \quad & \sum_{m\in\mathcal{M}}\sum_{t\in\mathcal{T}} W_m\Bigg[\sum_{n\in\mathcal{N}}\left(A_{m,n,t}c_{m,n,t}-\frac{1}{2}Z_{m,n,t}c^2_{m,n,t}\right)-\sum_{i\in\mathcal{I}}\sum_{n\in\mathcal{N}}\sum_{u\in\mathcal{U}_{i,n}} C^{\text{opr}}_u y_{i,m,n,t,u} \\
& -\sum_{i\in\mathcal{I}}\sum_{n\in\mathcal{N}} C^{\text{sto}} r^{\text{out}}_{i,m,n,t}\Bigg]-\sum_{i\in\mathcal{I}}\sum_{n\in\mathcal{N}}\sum_{u\in\mathcal{U}_{i,n}} C^{\text{ava}}_u a_{i,n,u}-\sum_{i\in\mathcal{I}}\sum_{n\in\mathcal{N}}\sum_{u\in\mathcal{U}_{i,n}} C^{\text{gen}}_u z_{i,n,u} \\
& -\sum_{j\in\mathcal{J}_\ell}\sum_{\ell\in\mathcal{L}} C^{\text{trn}}_{j,\ell}x_{j,\ell}-D\sum_{i\in\mathcal{I}}\sum_{m\in\mathcal{M}}\sum_{n\in\mathcal{N}}\sum_{t\in\mathcal{T}}\sum_{u\in\mathcal{U}_{i,n}} W_m F_u y_{i,m,n,t,u}
\end{aligned}
\tag{1a}
$$

$$\text{s.t.} \qquad x_{j,\ell} \in \{0,1\}, \forall \ell, j \in \mathcal{J}_\ell \tag{1b}$$

$$\sum_{j \in \mathcal{J}_\ell} x_{j,\ell} = 1, \forall \ell \tag{1c}$$

$$\begin{aligned} &-(1-x_{j,\ell})M^{\text{trn}} \leq f_{j,\ell,m,t} - B_{j,\ell}\left(v_{m,n_\ell^+,t} - v_{m,n_\ell^-,t}\right) \leq (1-x_{j,\ell})M^{\text{trn}}, \\ &\forall \ell, m, t, j \in \mathcal{J}_\ell \end{aligned} \tag{1d}$$

$$-T_t K^{\text{trn}}_{j,\ell} x_{j,\ell} \leq T_t f_{j,\ell,m,t} \leq T_t K^{\text{trn}}_{j,\ell} x_{j,\ell}, \forall \ell, m, t, j \in \mathcal{J}_\ell \tag{1e}$$

$$\hat{f}_{\ell,m,t} = \sum_{j \in \mathcal{J}_\ell} f_{j,\ell,m,t}, \forall \ell, m, t \tag{1f}$$

$$-\pi \leq v_{m,n,t} \leq \pi, \forall m, n, t \tag{1g}$$

$$T_t \underline{G}_{m,n,t,u} a_{i,n,u} \leq y_{i,m,n,t,u} \leq T_t \overline{G}_{m,n,t,u} a_{i,n,u}, \forall i, m, n, t, u \in \mathcal{U}_{i,n} \tag{1h}$$

$$y_{i,m,n,t,u} - y_{i,m,n,t-1,u} \leq T_t R^{\text{up}}_u a_{i,n,u}, \forall i, m, n, t \in \mathcal{T}^{\text{ini}}, u \in \mathcal{U}_{i,n} \tag{1i}$$

$$y_{i,m,n,t-1,u} - y_{i,m,n,t,u} \leq T_t R^{\text{down}}_u a_{i,n,u}, \forall i, m, n, t \in \mathcal{T}^{\text{ini}}, u \in \mathcal{U}_{i,n} \tag{1j}$$

$$a_{i,n,u} \leq K^{\text{gen}}_{i,n,u} + z_{i,n,u}, \forall i, n, u \in \mathcal{U}_{i,n} \tag{1k}$$

$$r^{\text{sto}}_{i,m,n,t} - \left(E^{\text{sto}}\right)^{T_t} r^{\text{sto}}_{i,m,n,t-1} - E^{\text{in}} r^{\text{in}}_{i,m,n,t} + r^{\text{out}}_{i,m,n,t} = 0, \forall i, m, n, t \in \mathcal{T}^{\text{ini}} \tag{1l}$$

$$r^{\text{sto}}_{i,m,n,t} - \left(E^{\text{sto}}\right)^{T_t} \underline{R}_{i,n} \overline{R}_{i,n} - E^{\text{in}} r^{\text{in}}_{i,m,n,t} + r^{\text{out}}_{i,m,n,t} = 0, \forall i, m, n, t \in \mathcal{T} \setminus \mathcal{T}^{\text{ini}} \tag{1m}$$

$$r^{\text{in}}_{i,m,n,t} \leq T_t R^{\text{in}} \overline{R}_{i,n}, \forall i, m, n, t \tag{1n}$$

$$r^{\text{out}}_{i,m,n,t} \leq T_t R^{\text{out}} \overline{R}_{i,n}, \forall i, m, n, t \tag{1o}$$

$$\underline{R}_{i,n} \overline{R}_{i,n} \leq r^{\text{sto}}_{i,m,n,t} \leq \overline{R}_{i,n}, \forall i, m, n, t \tag{1p}$$

$$\begin{aligned} c_{m,n,t} - \sum_{i \in \mathcal{I}} \sum_{u \in \mathcal{U}_{i,n}} y_{i,m,n,t,u} + VT_t \sum_{\ell \in \mathcal{L}_n^+} \hat{f}_{\ell,m,t} - VT_t \sum_{\ell \in \mathcal{L}_n^-} \hat{f}_{\ell,m,t} - \sum_{i \in \mathcal{I}} r^{\text{out}}_{i,m,n,t} \\ + \sum_{i \in \mathcal{I}} r^{\text{in}}_{i,m,n,t} = 0, \forall m, n, t \end{aligned} \tag{1q}$$

$$a_{i,n,u} \geq 0, \forall i, n, u \in \mathcal{U}_{i,n} \tag{1r}$$

$$c_{m,n,t} \geq 0, \forall m, n, t \tag{1s}$$

$$y_{i,m,n,t,u} \geq 0, \forall i, m, n, t, u \in \mathcal{U}_{i,n} \tag{1t}$$

$$z_{i,n,u} \geq 0, \forall i, n, u \in \mathcal{U}_{i,n} \tag{1u}$$

$$r^{\text{sto}}_{i,m,n,t} \geq 0, \forall i, m, n, t \tag{1v}$$

$$r^{\text{in}}_{i,m,n,t} \geq 0, \forall i, m, n, t \tag{1w}$$

$$r^{\text{out}}_{i,m,n,t} \geq 0, \forall i, m, n, t \tag{1x}$$

$$f_{j,\ell,m,t} \ \text{u.r.s.}, \forall \ell, m, t, j \in \mathcal{J}_\ell \tag{1y}$$

$$\hat{f}_{\ell,m,t} \ \text{u.r.s.}, \forall \ell, m, t \tag{1z}$$

$$v_{m,n,t} \ \text{u.r.s.}, \forall m, n, t \tag{1aa}$$

Decision variables include investments in transmission lines, adoption and availability of generation capacity, operation of PHS, generation output, transmission flows, and consumption, which comprise the set $\Omega^{\text{CP}} = \{a_{i,n,u}, c_{m,n,t}, f_{j,\ell,m,t}, \hat{f}_{\ell,m,t}, r^{\text{sto}}_{i,m,n,t}, r^{\text{in}}_{i,m,n,t}, r^{\text{out}}_{i,m,n,t}, v_{m,n,t}, x_{j,\ell}, y_{i,m,n,t,u}, z_{i,n,u}\}$.

The constraints include those related to transmission investment, viz., discrete selection of transmission capacity sizes for each line (1b) and exactly one discrete capacity level (including the existing one) is selected for each line (1c). Kirchhoff's laws are enforced by stipulating that transmission flow on each discrete capacity level of each line that is constructed is constrained by the product of the corresponding susceptance and nodal voltage-angle difference (1d). Power flows are constrained by the capacity limit for each discrete capacity level of each line that is constructed (1e). Realised power flow on each line is then simply the sum of the power flows on each discrete capacity level of the line (1f). Rounding out the transmission constraints, nodal voltage-angle differences must be bounded in order for the DC load-flow approximation to be adequate (1 g). Turning to power generation, it is subject to upper and lower limits based on availability factors and available capacity (1h). Its flexibility is governed by up- and down-ramping limits, (1i) and (1j), respectively, which are not applicable to the first period of each week. Meanwhile, available capacity is bounded by new and existing capacity (1k). As for storage, its energy-balance constraint states that end-of-period storage level equals the previous period's storage level plus the storage input minus the storage output inclusive of efficiency losses (1 l). Boundary conditions on storage operations during the initial period of each week are handled *via* the analogous expression (1 m). There are also restrictions on the rates at which storage can be charged and discharged, (1n) and (1o), respectively, along with minimum and maximum storage levels (1p). For the power system, the most crucial constraint is nodal energy balance, i.e. consumption must equal local generation and net storage output plus net energy import (1q). Last, we have non-negativity constraints on capacity availability, consumption, generation, storage decisions, and capacity investment (1r)–(1x), while power flows and voltage angles are 'unrestricted in sign' (1 y)–(1aa). The CP problem (1a)–(1aa) is a mixed-integer quadratic programming (MIQP) problem.[6]

3.2. Bi-level problem

The upper-level problem of the TSO is:

$$\begin{aligned}\underset{x_{j,\ell}}{\text{Maximise}}\quad & \sum_{m\in\mathcal{M}}\sum_{t\in\mathcal{T}} W_m\Bigg[\sum_{n\in\mathcal{N}}\left(A_{m,n,t}c_{m,n,t}-\frac{1}{2}Z_{m,n,t}c_{m,n,t}^2\right)-\sum_{i\in\mathcal{I}}\sum_{n\in\mathcal{N}}\sum_{u\in\mathcal{U}_{i,n}}C_u^{\text{opr}}y_{i,m,n,t,u}\\ & -\sum_{i\in\mathcal{I}}\sum_{n\in\mathcal{N}}C^{\text{sto}}r_{i,m,n,t}^{\text{out}}\Bigg]-\sum_{i\in\mathcal{I}}\sum_{n\in\mathcal{N}}\sum_{u\in\mathcal{U}_{i,n}}C_u^{\text{ava}}a_{i,n,u}-\sum_{i\in\mathcal{I}}\sum_{n\in\mathcal{N}}\sum_{u\in\mathcal{U}_{i,n}}C_u^{\text{gen}}z_{i,n,u}\\ & -\sum_{j\in\mathcal{J}_\ell}\sum_{\ell\in\mathcal{L}}C_{j,\ell}^{\text{trn}}x_{j,\ell}-D\sum_{i\in\mathcal{I}}\sum_{m\in\mathcal{M}}\sum_{n\in\mathcal{N}}\sum_{t\in\mathcal{T}}\sum_{u\in\mathcal{U}_{i,n}}W_mF_uy_{i,m,n,t,u}\end{aligned} \tag{2a}$$

$$\text{s.t.}\qquad x_{j,\ell}\in\{0,1\},\forall\ell,j\in\mathcal{J}_\ell \tag{2b}$$

$$\sum_{j\in\mathcal{J}_\ell}x_{j,\ell}=1,\forall\ell \tag{2c}$$

(2a)–(2c) are identical to (1a)–(1c), viz., (2a) maximises social welfare consisting of consumer surplus, producer surplus, merchandising surplus, the cost of transmission expansion, and the cost of damage from emissions. Meanwhile, (2b)–(2c) enforce the binary choice of transmission lines. However, unlike (1a), the only decision variable that is directly under the control of the TSO at the upper level is transmission investment, i.e. $x_{j,\ell}$. The set $\Omega^{\text{LL}}\equiv\{a_{i,n,u},c_{m,n,t},f_{j,\ell,m,t},\hat{f}_{\ell,m,t},r_{i,m,n,t}^{\text{sto}},r_{i,m,n,t}^{\text{in}},r_{i,m,n,t}^{\text{out}},\ v_{m,n,t},$ $y_{i,m,n,t,u},z_{i,n,u}\}$ comprises the lower-level decision variables that the TSO anticipates when investing in transmission lines but cannot directly affect.

The lower-level problem is expressed using the extended-cost function:[7]

$$\begin{aligned}\underset{\Omega^{\text{LL}}}{\text{Maximise}}\quad & \sum_{m\in\mathcal{M}}\sum_{t\in\mathcal{T}} W_m\Bigg[\sum_{n\in\mathcal{N}}\left(A_{m,n,t}c_{m,n,t}-\frac{1}{2}Z_{m,n,t}c_{m,n,t}^2\right)-\sum_{i\in\mathcal{I}}\sum_{n\in\mathcal{N}}\sum_{u\in\mathcal{U}_{i,n}}C_u^{\text{opr}}y_{i,m,n,t,u}\\ & -\sum_{i\in\mathcal{I}}\sum_{n\in\mathcal{N}}C^{\text{sto}}r_{i,m,n,t}^{\text{out}}\Bigg]-\sum_{i\in\mathcal{I}}\sum_{n\in\mathcal{N}}\sum_{u\in\mathcal{U}_{i,n}}C_u^{\text{gen}}z_{i,n,u}-\sum_{i\in\mathcal{I}}\sum_{n\in\mathcal{N}}\sum_{u\in\mathcal{U}_{i,n}}C_u^{\text{ava}}a_{i,n,u}\\ & -\frac{1}{2}\sum_{m\in\mathcal{M}}\sum_{n\in\mathcal{N}}\sum_{t\in\mathcal{T}}W_mZ_{m,n,t}\sum_{i\in\mathcal{I}}\left(\sum_{u\in\mathcal{U}_{i,n}}y_{i,m,n,t,u}+r_{i,m,n,t}^{\text{out}}-r_{i,m,n,t}^{\text{in}}\right)^2\\ & -HD\sum_{i\in\mathcal{I}}\sum_{m\in\mathcal{M}}\sum_{n\in\mathcal{N}}\sum_{t\in\mathcal{T}}\sum_{u\in\mathcal{U}_{i,n}}W_mF_uy_{i,m,n,t,u}\end{aligned} \tag{3a}$$

$$\text{s.t.} \qquad f_{j,\ell,m,t} = x_{j,\ell} B_{j,\ell}\left(v_{n_\ell^+,m,t} - v_{n_\ell^-,m,t}\right): \ \mu_{j,\ell,m,t}, \forall \ell, m, t, j \in \mathcal{J}_\ell \tag{3b}$$

$$\underline{\mu}_{j,\ell,m,t} \ : -T_t K^{\text{trn}}_{j,\ell} \le T_t f_{j,\ell,m,t} \le T_t K^{\text{trn}}_{j,\ell}: \ \overline{\mu}_{j,\ell,m,t}, \forall \ell, m, t, j \in \mathcal{J}_\ell \tag{3c}$$

$$\hat{f}_{\ell,m,t} = \sum_{j \in \mathcal{J}_\ell} f_{j,\ell,m,t}: \ \psi_{\ell,m,t}, \forall \ell, m, t \tag{3d}$$

$$\underline{\kappa}_{m,n,t} \ : -\pi \le v_{m,n,t} \le \pi: \ \overline{\kappa}_{m,n,t}, \forall m, n, t \tag{3e}$$

$$\underline{\beta}_{i,m,n,t,u} \ : T_t \underline{G}_{m,n,t,u} a_{i,n,u} \le y_{i,m,n,t,u} \le T_t \overline{G}_{m,n,t,u} a_{i,n,u} : \overline{\beta}_{i,m,n,t,u}, \forall i, m, n, t, u \in \mathcal{U}_{i,n} \tag{3f}$$

$$y_{i,m,n,t,u} - y_{i,m,n,t-1,u} \le T_t R^{\text{up}}_u a_{i,n,u}: \ \beta^{\text{up}}_{i,m,n,t,u}, \forall i, m, n, t \in \mathcal{T}^{\text{ini}}, u \in \mathcal{U}_{i,n} \tag{3g}$$

$$y_{i,m,n,t-1,u} - y_{i,m,n,t,u} \le T_t R^{\text{down}}_u a_{i,n,u}: \ \beta^{\text{down}}_{i,m,n,t,u}, \forall i, m, n, t \in \mathcal{T}^{\text{ini}}, u \in \mathcal{U}_{i,n} \tag{3h}$$

$$a_{i,n,u} \le K^{\text{gen}}_{i,n,u} + z_{i,n,u}: \ \beta^{\text{ava}}_{i,n,u}, \forall i, n, u \in \mathcal{U}_{i,n} \tag{3i}$$

$$r^{\text{sto}}_{i,m,n,t} - \left(E^{\text{sto}}\right)^{T_t} r^{\text{sto}}_{i,m,n,t-1} - E^{\text{in}} r^{\text{in}}_{i,m,n,t} + r^{\text{out}}_{i,m,n,t} = 0: \ \theta^{\text{sto}}_{i,m,n,t}, \forall i, m, n, t \in \mathcal{T}^{\text{ini}} \tag{3j}$$

$$r^{\text{sto}}_{i,m,n,t} - \left(E^{\text{sto}}\right)^{T_t} \underline{R}_{i,n} \overline{R}_{i,n} - E^{\text{in}} r^{\text{in}}_{i,m,n,t} + r^{\text{out}}_{i,m,n,t} = 0: \ \theta^{\text{sto}}_{i,m,n,t}, \forall i, m, n, t \in \mathcal{T} \setminus \mathcal{T}^{\text{ini}} \tag{3k}$$

$$r^{\text{in}}_{i,m,n,t} \le T_t R^{\text{in}} \overline{R}_{i,n}: \ \theta^{\text{in}}_{i,m,n,t}, \forall i, m, n, t \tag{3l}$$

$$r^{\text{out}}_{i,m,n,t} \le T_t R^{\text{out}} \overline{R}_{i,n}: \ \theta^{\text{out}}_{i,m,n,t}, \forall i, m, n, t \tag{3m}$$

$$\underline{\theta}_{i,m,n,t} \ : \underline{R}_{i,n} \overline{R}_{i,n} \le r^{\text{sto}}_{i,m,n,t} \le \overline{R}_{i,n}: \ \overline{\theta}_{i,m,n,t}, \forall i, m, n, t \tag{3n}$$

$$\begin{aligned} c_{m,n,t} - \sum_{i \in \mathcal{I}} \sum_{u \in \mathcal{U}_{i,n}} y_{i,m,n,t,u} + VT_t \sum_{\ell \in \mathcal{L}_n^+} \hat{f}_{\ell,m,t} - VT_t \sum_{\ell \in \mathcal{L}_n^-} \hat{f}_{\ell,m,t} - \sum_{i \in \mathcal{I}} r^{\text{out}}_{i,m,n,t} \\ + \sum_{i \in \mathcal{I}} r^{\text{in}}_{i,m,n,t} = 0: \ \lambda_{m,n,t}, \forall m, n, t \end{aligned} \tag{3o}$$

$$a_{i,n,u} \ge 0: \ \phi^a_{i,n,u}, \forall i, n, u \in \mathcal{U}_{i,n} \tag{3p}$$

$$c_{m,n,t} \ge 0: \ \phi^c_{m,n,t}, \forall m, n, t \tag{3q}$$

$$y_{i,m,n,t,u} \ge 0: \ \phi^y_{i,m,n,t,u}, \forall i, m, n, t, u \in \mathcal{U}_{i,n} \tag{3r}$$

$$z_{i,n,u} \geq 0: \quad \phi^{z}_{i,n,u}, \forall i, n, u \in \mathcal{U}_{i,n} \tag{3s}$$

$$r^{\text{sto}}_{i,m,n,t} \geq 0: \quad \phi^{\text{sto}}_{i,m,n,t}, \forall i, m, n, t \tag{3t}$$

$$r^{\text{in}}_{i,m,n,t} \geq 0: \quad \phi^{\text{in}}_{i,m,n,t}, \forall i, m, n, t \tag{3u}$$

$$r^{\text{out}}_{i,m,n,t} \geq 0: \quad \phi^{\text{out}}_{i,m,n,t}, \forall i, m, n, t \tag{3v}$$

$$f_{j,\ell,m,t} \text{ u.r.s.}, \forall \ell, m, t, j \in \mathcal{J}_{\ell} \tag{3w}$$

$$\hat{f}_{\ell,m,t} \text{ u.r.s.}, \forall \ell, m, t \tag{3x}$$

$$v_{m,n,t} \text{ u.r.s.}, \forall m, n, t \tag{3y}$$

The objective function (3a) includes all of the welfare terms from the upper-level objective function (2a) with two modifications. First, the cost of damage is scaled by parameter $H \in [0, 1]$, which specifies the extent of carbon taxation at the lower level. Second, the extended-cost term, $-\frac{1}{2}\sum_{m\in\mathcal{M}}\sum_{n\in\mathcal{N}}\sum_{t\in\mathcal{T}} W_m Z_{m,n,t} \sum_{i\in\mathcal{I}}\left(\sum_{u\in\mathcal{U}_{i,n}} y_{i,m,n,t,u} + r^{\text{out}}_{i,m,n,t} - r^{\text{in}}_{i,m,n,t}\right)^2$, is included to model a Cournot oligopoly and excluded otherwise. Constraints (3b)–(3c) are similar to (1d)–(1e) from central planning. Since $x_{j,\ell}$ is not a decision variable at the lower level, (3b) does not require linearisation as per (1d)–(1e). The remaining constraints, (3d)–(3y), are identical to (1f)–(1aa) from central planning. Finally, the lower-case Greek letters in colons next to the constraints are the corresponding dual variables.

3.3. Mathematical program with primal and dual constraints

The MPPDC resolution of the bi-level problem corresponding to the TSO's sustainable transmission expansion in a restructured electricity industry is:

$$\begin{aligned} \underset{\{x_{j,\ell}\}\cup\Omega^{\text{LL}}\cup\Omega^{\text{DV}}}{\text{Maximise}} \quad & (2a) \\ \text{s.t.} \quad & (2b)-(2c) \\ & (3b)-(3y) \\ & (\text{B-1a})-(\text{B-1t}) \\ & (\text{B-3a}) \end{aligned}$$

where $\Omega^{\text{DV}} \equiv \{\beta^{\text{ava}}_{i,n,u}, \underline{\beta}_{i,m,n,t,u}, \overline{\beta}_{i,m,n,t,u}, \phi^{a}_{i,n,u}, \phi^{y}_{i,m,n,t,u}, \phi^{z}_{i,n,u}, \underline{\mu}_{j,\ell,m,t}, \overline{\mu}_{j,\ell,m,t}, \underline{\kappa}_{m,n,t}, \overline{\kappa}_{m,n,t}, \phi^{c}_{m,n,t}, \lambda_{m,n,t}, \mu_{j,\ell,m,t}, \hat{\mu}_{j,\ell,m,t}, \psi_{\ell,m,t}, \beta^{\text{down}}_{i,m,n,t,u}, \beta^{\text{up}}_{i,m,n,t,u}, \theta^{\text{sto}}_{i,m,n,t}, \theta^{\text{in}}_{i,m,n,t}, \theta^{\text{out}}_{i,m,n,t}, \underline{\theta}_{i,m,n,t}, \overline{\theta}_{i,m,n,t}, \phi^{\text{sto}}_{i,m,n,t}, \phi^{\text{in}}_{i,m,n,t}, \phi^{\text{out}}_{i,m,n,t}\}$ comprises the dual variables from the lower level.[8] This MPPDC is nonlinear because of bilinear terms $x_{j,\ell}(v_{n^+_{\ell},m,t} - v_{n^-_{\ell},m,t})$

and $x_{j,\ell}\mu_{j,\ell,m,t}$ in (3b) and (B-1i), respectively. Indeed, although $x_{j,\ell}$ is not a decision variable at the lower level, it is one for the MPPDC as a whole.

3.4. Mixed-Integer quadratically constrained quadratic program

We linearise the MPPDC by first replacing (3b)–(3c) by (1d)–(1e) as in the central-planning MIQP. As for (B-1i), we linearise it *via* the auxiliary variable $\hat{\mu}_{j,\ell,m,t}$ as follows:

$$-\sum_{\ell\in\mathcal{L}_n^+}\sum_{j\in\mathcal{J}_\ell}B_{j,\ell}\left(\mu_{j,\ell,m,t}-\hat{\mu}_{j,\ell,m,t}\right)+\sum_{\ell\in\mathcal{L}_n^-}\sum_{j\in\mathcal{J}_\ell}B_{j,\ell}\left(\mu_{j,\ell,m,t}-\hat{\mu}_{j,\ell,m,t}\right)+\overline{\kappa}_{m,n,t}-\underline{\kappa}_{m,n,t}=0,\quad \forall m,n,t \tag{5a}$$

$$-x_{j,\ell}M^{\mathrm{trn}}\leq\mu_{j,\ell,m,t}-\hat{\mu}_{j,\ell,m,t}\leq x_{j,\ell}M^{\mathrm{trn}},\forall\ell,m,t,j\in\mathcal{J}_\ell \tag{5b}$$

$$-(1-x_{j,\ell})M^{\mathrm{trn}}\leq\hat{\mu}_{j,\ell,m,t}\leq(1-x_{j,\ell})M^{\mathrm{trn}},\forall\ell,m,t,j\in\mathcal{J}_\ell \tag{5c}$$

$$\hat{\mu}_{j,\ell,m,t}\ \text{u.r.s.},\forall\ell,m,t,j\in\mathcal{J}_\ell \tag{5d}$$

Hence, the MIQCQP is:

$$\begin{aligned}\underset{\{x_{j,\ell}\}\cup\Omega^{\mathrm{LL}}\cup\Omega^{\mathrm{DV}}}{\text{Maximise}}\quad & (2a)\\ \text{s.t.}\quad & (2b)-(2c)\\ & (1d)-(1e),\quad (3d)-(3y)\\ & (B\text{-}1a)-(B\text{-}1f),\quad (B\text{-}1h),\quad (5a)-(5d)\\ & (B\text{-}3a)\end{aligned}$$

4. Numerical examples

We tackle RQs 1–2 *via* numerical examples. The impact of market structure and emission intensities of generation portfolios is addressed by comparing the results of the illustrative greenfield example and the brownfield Western European case study in Sections 4.1 and 4.2, respectively. In effect, we explore how changes to D and H affect power-system outcomes. These parameters reflect the exogenous combinations of social cost of damage and CO_2 pricing that may arise in future power systems.

4.1. Illustrative Greenfield example

4.1.1. Data

An illustrative example is implemented for a greenfield three-node test network with three candidate lines (Figure 1). There are two firms, $i1$ and $i2$, which have the possibility of investing in coal-, gas-, and wind-generation capacity at nodes $n1$, $n2$, and

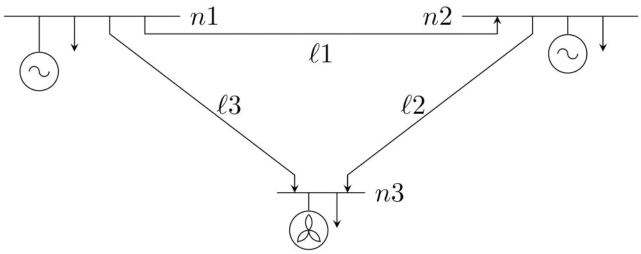

Figure 1. Greenfield test network.

Table 1. Greenfield transmission-line parameters for all ℓ.

Level \ Attribute	$B_{j,\ell}$	$K^{\text{trn}}_{j,\ell}$	$C^{\text{trn}}_{j,\ell}$
$j1$	0	0	0
$j2$	1,500	6.1	48
$j3$	2,000	18.3	96
$j4$	2,800	30.5	216
$j5$	4,900	42.7	288
$j6$	5,400	54.9	360

Table 2. Greenfield emission rates [t/MWh], operating costs [€/MWh], amortised investment costs [€/MW], amortised fixed O&M costs [€/MW], and ramp rates [–].

Technology \ Attribute	F_u	C^{opr}_u	C^{gen}_u	C^{ava}_u	$R^{\text{up}}_u = R^{\text{down}}_u$
$u1$	0.9	20	653.28	111.12	0.2
$u2$	0.5	35	192.72	38.64	0.5
$u3$	0	0	224.88	72.24	1

$n3$, respectively. We assume that firm $i1$ has the 'brown' portfolio at nodes $n1$–$n2$ and firm $i2$ has the 'green' portfolio at node $n3$. Apart from a modest amount of storage capacity at node $n2$ belonging to firm $i2$, there is no initial generation or transmission capacity, i.e. this is a greenfield example. There are four equally weighted representative days (instead of weeks here), i.e. $W_m = \frac{1}{4}$, and 24 time periods per day, i.e. $|\mathcal{M}| = 4$ and $|\mathcal{T}| = 24$. The TSO can invest in exactly one discrete capacity level per line with characteristics given in Table 1 (Maurovich-Horvat et al. 2015). In particular, the cost, $C^{\text{trn}}_{j,\ell}$, is on a daily basis for a notional 1-km line, which means an annualised cost of €17,520 to €131,400 for levels $j2$ to $j6$, respectively, i.e. approximately €2,500/MW-km.

Data for generation units are given in Table 2, where $u1$, $u2$, and $u3$ correspond to coal, gas, and wind, respectively.[9] For example, the overnight capital cost of a 650 MW coal plant is \$3,676/kW, which annualises to \$239.12/kW assuming a 5% per annum interest rate and a thirty-year lifetime. Subsequently, this becomes an hourly cost of \$27.22/MWh, which is approximately the €653.28/MW daily capital cost used here. Likewise, the daily capital costs for gas and wind technologies are based on the overnight capital costs of a 430 MW CCGT plant and a 200 MW onshore wind plant, viz., \$1,084/kW and \$1,265/kW, respectively.[10] Operating costs are loosely based on the same source and exclude costs of CO_2 emission permits. Meanwhile, the annual fixed O&M cost of a 650 MW coal plant is \$40.58/kW, which becomes an hourly cost of \$4.63/MWh. Thus, we have a daily fixed O&M cost for

Table 3. Greenfield base demand parameters for all (m, t).

Parameter \ Node	$n1$	$n2$	$n3$
$A_{m,n,t}$	200	175	125
$Z_{m,n,t}$	1	1	1

Table 4. Numerical results for greenfield PC instances with $H = 0$ (in k€ unless indicated).

Metric \ D	0	25	50	75	100
SW	597.80	468.41	341.85	222.52	110.09
CS	570.38	556.35	551.12	544.98	544.98
PS	0	0	0	0	0
MS	28.50	40.23	36.99	15.23	15.23
GR	0	0	0	0	0
DC	0	127.44	245.57	337.28	449.71
TP	1.08	0.72	0.70	0.41	0.41
EM (kt)	5.63	5.10	4.91	4.50	4.50
GC (MW)	[133 229 0]	[99 246 43]	[98 233 95]	[99 196 229]	[99 196 229]
TC (MW)	[54.9 54.9 54.9]	[54.9 54.9 0]	[54.9 42.7 6.1]	[54.9 6.1 0]	[54.9 6.1 0]

coal of €111.12/MW. In a similar vein, the annual fixed O&M costs of a 430 MW combined-cycle gas-fired plant and a 200 MW on-shore wind plant, viz., \$14.10/kW and \$26.34/kW, become daily fixed O&M costs of €38.64/MW and €72.24/MW, respectively. Finally, the ramp rates are representative with the understanding that wind output is uncontrollable and determined by availability of resources.

Base demand parameters indicate that node $n1$ is the load centre, while node $n3$ has relatively low demand (Table 3). The $A_{m,n,t}$ values vary during the day, i.e. increasing by noon and decreasing thereafter back to their base levels by midnight. By contrast, node $n3$ has the potential for wind adoption with base availabilities of 0.50 and 0.25 in days $m1$ (and $m3$) and $m2$ (and $m4$), respectively, with oscillations from these baselines throughout the day.[11] Finally, there is $\overline{R}_{i,n} = 0.6$ MW of storage capacity at node $n2$ belonging to firm $i2$ with $C^{\mathrm{sto}} = 0$, $E^{\mathrm{sto}} = 1$, $E^{\mathrm{in}} = 0.75$, $R^{\mathrm{in}}_{i,n} = R^{\mathrm{out}}_{i,n} = 0.16$, and $\underline{R}_{i,n} = 0.3$, which is also the initial state of charge, cf. Virasjoki et al. (2020).

4.1.2. Solution approach

We implement the MIQCQP problem instances for H values between 0 and 1 and D values between €0/t and €100/t. Since the PC problem instances with $H = 1$ are identical to the MIQP CP problem instances, we report merely the PC results. All problem instances take a few seconds to solve to optimality with GAMS 40.3.0 using Gurobi library version 9.5.2 deployed on a 12th Generation Intel(R) Core(TM) i7-1280P 1.80 GHz 12-core processor and 32.0 GB of RAM.

4.1.3. Perfect competition

The PC results are given in Tables 4–6, where 'CS' refers to consumer surplus, 'PS' refers to producer surplus, 'MS' refers to the ISO's merchandising surplus, 'TP' refers to the TSO's amortised cost of transmission investment, 'DC' refers to the social cost of damage from CO_2 emissions, 'EM' refers to CO_2 emissions, 'GC' refers to generation capacity adopted at each node, and 'TC' refers to transmission capacity adopted for each line. The calculations of these welfare components are explained in Supplementary Appendix D. As a benchmark, we first explore the findings in Table 6

Table 5. Numerical results for greenfield PC instances with $H = 0.50$ (in k€ unless indicated).

Metric \ D	0	25	50	75	100
SW	597.80	474.38	373.43	309.46	260.14
CS	570.38	496.26	436.22	385.24	333.62
PS	0	0	0	0	0
MS	28.50	38.58	38.45	45.18	60.34
GR	0	59.75	100.23	119.89	132.73
DC	0	119.49	200.46	239.78	265.47
TP	1.08	0.72	1.01	1.08	1.08
EM (kt)	5.63	4.78	4.01	3.20	2.65
GC (MW)	[133 229 0]	[88 239 43]	[64 217 171]	[37 201 315]	[20 188 363]
TC (MW)	[54.9 54.9 54.9]	[54.9 54.9 0]	[54.9 42.7 54.9]	[54.9 54.9 54.9]	[54.9 54.9 54.9]

Table 6. Numerical results for greenfield PC instances with $H = 1$ (in k€ unless indicated).

Metric \ D	0	25	50	75	100
SW	597.80	476.37	392.87	337.48	292.77
CS	570.38	440.21	333.62	264.43	233.33
PS	0	0	0	0	0
MS	28.50	36.88	60.34	74.14	60.52
GR	0	111.53	132.73	145.37	163.14
DC	0	111.53	132.73	145.37	163.14
TP	1.08	0.72	1.08	1.08	1.08
EM (kt)	5.63	4.46	2.65	1.94	1.63
GC (MW)	[133 229 0]	[77 233 44]	[20 188 363]	[0 166 419]	[0 150 472]
TC (MW)	[54.9 54.9 54.9]	[54.9 54.9 0]	[54.9 54.9 54.9]	[54.9 54.9 54.9]	[54.9 54.9 54.9]

because $H = 1$ under PC is equivalent to the first-best CP result. For $D = 0$, it is optimal to invest in coal and gas capacity and to build all lines to transmit power to node $n3$. Indeed, absent a damage cost, it is not economical to invest in wind. For $D = 25$, flow on line $\ell 1$ increases in absolute terms to send more gas-generated power from node $n2$ to $n1$. At the same time, line $\ell 3$ is removed to limit coal generation with a role for wind. Only when $D = 50$ does wind enter the generation mix with a substantial capacity to render node $n3$ into a net exporter. Naturally, this change in the generation mix has consequences for transmission planning as line $\ell 3$ is added to facilitate imports at node $n1$. At a tipping point of $D = 75$, the cost of damage from emissions is high enough to eliminate coal and to reduce gas capacity, although node $n2$ remains a net exporter including to node $n3$ on line $\ell 2$. Finally, for $D = 100$, the capacity of gas generation decreases as node $n3$ imports less power from node $n2$.

As a contrast, the result with $H = 0$ under PC in Table 4 excludes any internalisation of the cost of damage from CO_2 emissions. Thus, consumers have no incentive to curb quantity demanded when D increases as in the case with $H = 1$. Instead, the TSO takes a countervailing decision to reduce transmission capacity by drastically limiting line $\ell 2$ and removing line $\ell 3$ when $D \geq 75$. Although such a topology induces modest adoption of wind capacity at node $n3$ when $D = 75$, it does not enable substantial cuts in CO_2 emissions because prices are not high enough to entice additional wind capacity at node $n3$. Consequently, CO_2 emissions remain stuck at 4.50 kt no matter how much D increases.

A partial measure with $H = 0.50$ under PC in Table 5 enables half of the cost of damage from emissions to be internalised, which means that the network topology starts to resemble the socially optimal one in Table 6. Nevertheless, there are some subtle differences. For example, for $D = 50$, there is actually less transmission capacity adopted with $H = 0.50$ than with $H = 1$. This is because consumption is not sufficiently curtailed, which limits the potential for wind power to be exported from node $n3$. Furthermore, coal is never eliminated even for $D = 100$. Hence, we address RQ 1 by noting that the reduction in SW for $H = 0$ is relatively high when D goes from €50/t to €100/t *ceteris paribus* compared to the cases for $H = 0.50$ and $H = 1$ because the latter enable the system to curtail consumption to mitigate the DC and to tailor transmission capacity accordingly.

4.1.4. Cournot oligopoly

Contrary to the PC results, those under CO exhibit adoption of generation capacity at all nodes for all values of D and H (Tables 7–9). This is because the exertion of market power by both firms leads to high prices and anticipative transmission investment by the TSO to mitigate welfare loss (Sauma and Oren 2006). With $H = 0$ (see Table 7), only lines $\ell 1$ and $\ell 3$ are built for $D = 0$ with power exported from nodes $n2$ and $n3$ to $n1$. Given the possibility of high prices, it is profitable to invest in wind already. When $D = 25$, both coal and gas capacities shrink. These decisions are driven by the TSO's addition of line $\ell 2$ and expansion of line $\ell 3$ with elimination of line $\ell 1$ to limit coal generation. Accordingly, wind capacity increases to meet some consumption at node $n1$. However, CO_2 emissions are not possible to reduce any further, which leads to sustained decreases in welfare as D increases *ceteris paribus* to €100/t. Interestingly, for $D \geq 75$, the SW under CO actually exceeds that under PC, cf. Table 4, because market power curbs the DC from CO_2 emissions.

While internalisation of the cost of damage from emissions is monotonically welfare enhancing under PC, it is not the case under CO, which addresses RQ 2. This is

Table 7. Numerical results for greenfield CO instances with $H = 0$ (in k€ unless indicated).

Metric \ D	0	25	50	75	100
SW	411.48	354.20	297.71	241.23	184.74
CS	141.20	150.43	150.43	150.43	150.43
PS	268.95	260.65	260.65	260.65	260.65
MS	1.47	0	0	0	0
GR	0	0	0	0	0
DC	0	56.49	112.98	169.47	225.95
TP	0.14	0.38	0.38	0.38	0.38
EM (kt)	2.38	2.26	2.26	2.26	2.26
GC (MW)	[68 75 130]	[65 72 170]	[65 72 170]	[65 72 170]	[65 72 170]
TC (MW)	[18.3 0 6.1]	[0 18.3 42.7]	[0 18.3 42.7]	[0 18.3 42.7]	[0 18.3 42.7]

Table 8. Numerical results for greenfield CO instances with $H = 0.50$ (in k€ unless indicated).

Metric \ D	0	25	50	75	100
SW	411.48	343.24	285.89	238.46	200.56
CS	141.20	138.39	126.81	115.45	104.66
PS	268.95	230.87	205.53	184.66	168.17
MS	1.47	0.01	0	0.14	0.03
GR	0	25.58	45.91	61.23	71.55
DC	0	51.16	91.82	122.45	143.11
TP	0.14	0.46	0.55	0.55	0.74
EM (kt)	2.38	2.05	1.84	1.63	1.43
GC (MW)	[68 75 130]	[57 69 180]	[49 66 191]	[41 63 200]	[33 61 210]
TC (MW)	[18.3 0 6.1]	[0 18.3 54.9]	[18.3 18.3 54.9]	[18.3 18.3 54.9]	[18.3 42.7 54.9]

Table 9. Numerical results for greenfield CO instances with $H = 1$ (in k€ unless indicated).

Metric \ D	0	25	50	75	100
SW	411.48	331.82	272.11	230.24	203.87
CS	141.20	126.74	104.66	84.23	64.75
PS	268.95	205.41	168.17	146.63	136.65
MS	1.47	0.13	0.03	0.39	3.55
GR	0	45.94	71.55	77.95	67.00
DC	0	45.94	71.55	77.95	67.00
TP	0.14	0.46	0.74	1.01	1.08
EM (kt)	2.38	1.84	1.43	1.04	0.67
GC (MW)	[68 75 130]	[49 66 190]	[33 61 210]	[18 56 231]	[3 52 249]
TC (MW)	[18.3 0 6.1]	[0 18.3 54.9]	[18.3 42.7 54.9]	[42.7 54.9 54.9]	[54.9 54.9 54.9]

because there is also the distortion from market power, and, for relatively low levels of D, the reduction in DC is more than offset by the loss in CS as consumption is choked off further. This is precisely the case for $H = 0.50$ when $D < 100$ (see Table 8). For example, the TSO increases the capacity of line $\ell 3$ vis-à-vis $H = 0$ for $D = 25$ in order to incentivise the wind plant to export to node $n1$. Nevertheless, when $D = 50$, further expansion to wind capacity requires the addition of line $\ell 1$ as wind's exports are routed *via* node $n2$. When $D = 100$, the capacity of line $\ell 2$ is augmented in order to reduce coal capacity further. Interestingly, this is also the point at which the incorporation of a (partial) carbon charge actually improves maximised SW, cf. Table 7. A full internalisation of the cost of damage from emissions with $H = 1$ as in Table 9 leads to the 'terminal' network topology under $H = 0.50$ with construction of all three lines at a higher capacity for $D = 50$. In effect, the TSO incentivises additional wind capacity in order to maintain CS and PS. Hence, in contrast to PC, internalisation of the cost of damage from emissions under CO may actually be welfare reducing for low D.

4.2. Brownfield Western European case study

4.2.1. Data

The case study is based on a 15-node and 28-line Western European test network (Neuhoff et al. 2005). For computational tractability, the test network is devised of four national nodes, viz., Germany ($n1$), France ($n2$), Belgium ($n3$), and the Netherlands ($n4$), and four existing cross-border lines, which can be upgraded in capacity, plus two candidate lines indicated by the dashed arcs in Figure 2. A given test year (2017) is reduced to four representative weeks ($m \in \mathcal{M}$) each comprising 168 h ($t \in \mathcal{T}$) *via* a clustering procedure that reflects the system's spatio-temporal texture. By taking the observed consumption and VRE availability data as inputs, the clustering procedure of Virasjoki et al. (2020) selects weeks 6 ($m1$), 18 ($m2$), 20 ($m3$), and 47 ($m4$) with relative weights, W_m, 7/52, 12/52, 23/52, and 10/52, respectively. These representative weeks capture seasonal conditions, e.g. high consumption and low solar availability during colder weeks $m1$ and $m4$ and vice versa for warmer weeks $m2$ and $m3$ (Figures 3 and 4). Furthermore, seasons may exhibit either high (weeks $m2$ and $m4$) or low (weeks $m1$ and $m3$) wind availability.

Generating units' characteristics, generation capacities, demand parameters, and PHS capacities are also based on 2017 data from Virasjoki et al. (2020). In particular,

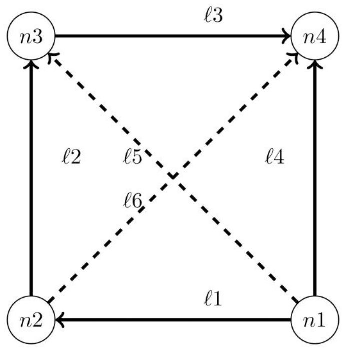

Figure 2. Western European test network.

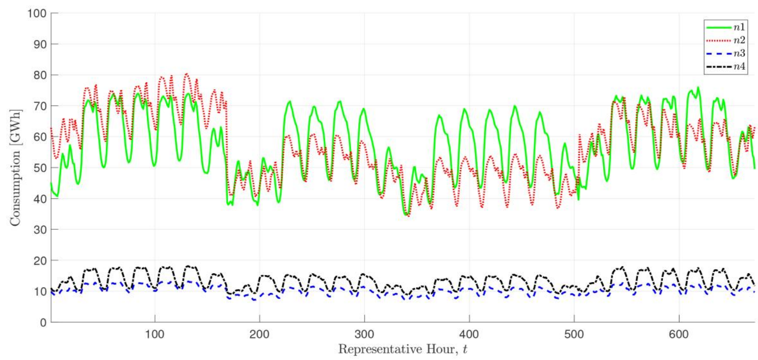

Figure 3. Nodal consumption data in representative weeks.

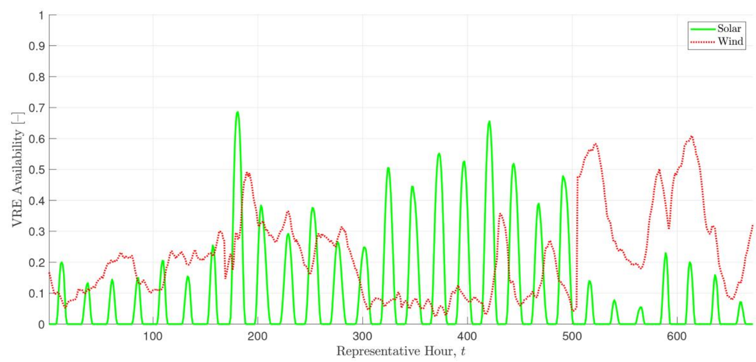

Figure 4. VRE availability data for *n*1 (Germany) in representative weeks.

Tables 10 and 11 indicate generating units' financial/technical attributes and firms' installed portfolios, respectively.[12] Inverse-demand functions' intercepts, $A_{m,n,t}$, and slopes, $Z_{m,n,t}$, are calculated using a point elasticity of -0.25 *via* the point-slope equation for a line that passes through the reference quantity/price pair for each node in each hour of the representative weeks. Meanwhile, PHS capacities, $\overline{R}_{i,n}$, are distributed as follows: *n*1: 6.6 GWh (Uniper), 10.7 GWh (RWE), 0.8 GWh (EnBW), 16.6 GWh (Vattenfall), 9.5 (FringeD); *n*2: 33.7 GWh (EDF); and *n*3: 6.7 GWh

Table 10. Operating costs [€/MWh], amortised investment costs [€/MW], amortised fixed O&M costs [€/MW], emission rates [t/MWh], and ramp rates [–].

Unit	C_u^{opr}	C_u^{gen}	C_u^{ava}	F_u	$R_u^{\text{up}} = R_u^{\text{down}}$
Nuclear *u*1	9.0	–	2333	0.00	0.1
Lignite *u*2	11.2	4573	778	0.94	0.1
Coal *u*3	27.4	4573	778	0.83	0.2
CCGT *u*4	31.6	1349	271	0.37	0.3
Gas *u*5	43.0	887	134	0.50	0.3
Oil *u*6	76.6	1680	271	0.72	0.7
Hydro *u*7	0.0	–	573	0.00	0.3
Solar *u*8	0.0	1638	292	0.00	1.0
Wind *u*9	0.0	1574	505	0.00	1.0

Table 11. Firms' installed capacities, $K_{i,n,u}^{\text{gen}}$ [GW], by node and unit.

Node	Firm	*u*1	*u*2	*u*3	*u*4	*u*5	*u*6	*u*7	*u*8	*u*9
*n*1	Uniper	–	0.9	3.2	2.7	0.5	1.2	–	–	0.3
	RWE	2.6	9.1	2.8	2.5	1.7	–	0.3	–	0.3
	EnBW	2.7	0.9	3.0	0.4	–	0.4	0.2	–	0.3
	Vattenfall	–	–	2.9	0.6	0.9	0.1	–	–	0.6
	FringeD	4.2	7.4	9.3	10.9	2.2	0.4	1.3	40.1	54.6
*n*2	EDF	63.1	–	4.0	1.4	–	7.0	15.0	0.3	1.5
	FringeF	–	–	–	3.8	2.4	–	3.6	6.5	12.3
*n*3	Electrabel	5.9	–	–	1.6	1.4	–	–	–	0.5
	EDF	–	–	–	0.4	0.4	–	–	–	0.1
	FringeB	–	–	–	1.0	–	–	–	3.3	2.1
*n*4	Electrabel	–	–	–	2.9	0.1	–	–	–	–
	Essent/RWE	–	–	1.4	1.9	0.6	–	–	–	–
	Nuon/Vattenfall	–	–	0.9	3.1	1.1	–	–	–	–
	FringeN	0.5	–	2.9	3.1	0.7	–	–	2.0	4.4

(Electrabel). PHS is assumed to have input efficiency, E^{in}, of 0.75, maximum charging/discharging rates, $R_{i,n}^{\text{in}} = R_{i,n}^{\text{out}}$, of 0.16, and minimum state of charge, $\underline{R}_{i,n}$, of 0.3. We also assume no PHS operating costs and zero self discharge.

Some differences from Virasjoki et al. (2020) are that we remove the cost of CO_2 emissions from generating units' operating costs to allow for explicit internalisation of the cost of damage from emissions *via* the D and H parameters. We also incorporate costs of investment in generation capacity along with amortised fixed O&M costs for available generation capacity.[13] For example, the overnight capital cost of a 650 MW coal plant is \$3,676/kW, which annualises to €237,794/MW (or, €4,573/MW on a weekly basis as indicated in Table 10) assuming a 5% per annum interest rate and a thirty-year lifetime. Likewise, the annual capital costs for CCGT and wind technologies are based on the overnight capital costs of a 430 MW CCGT plant and a 200 MW on-shore wind plant, viz., \$1,084/kW and \$1,265/kW, respectively.[14] These annualise to €70,510/MW (or, €1,349/MW on a weekly basis) and €82,290/MW (or, €1,574/MW on a weekly basis), respectively, using the aforementioned amortisation factors. Meanwhile, the annual fixed O&M cost of a 650 MW coal plant is \$40.58/kW, which becomes €40,580/MW (or, €778/MW on a weekly basis). In a similar vein, the annual fixed O&M costs of a 430 MW CCGT plant and a 200 MW on-shore wind plant, viz., \$14.10/kW and \$26.34/kW, become annual fixed O&M costs of €14,100/MW (or, €271/MW on a weekly basis) and €26,340/MW (or, €505/MW on a weekly basis), respectively. Capacity expansion in nuclear and hydro is not possible due to limited suitable sites.

The TSO can invest in exactly one discrete capacity level per line with characteristics given in Table 12 (Maurovich-Horvat et al. 2015). In particular, the cost, $C^{\text{trn}}_{j,\ell}$, is given on a weekly basis with two investment levels considered for each line, viz., $j1$ and $j2$ as the existing level and a 400 MW increase in capacity, respectively. We calculate susceptances based on flying distances between major cities of the four nodes (Egerer 2016; Rodríguez-Sarasty et al. 2021). Our annual amortised transmission-investment costs range from €287/MW-km to €575/MW-km.

4.2.2. Solution approach

Since the MIQCQP implementation is not tractable for the case study, we resort to enumerating all feasible transmission plans, i.e. $2^6 = 64$, and solving lower-level QP problem instances for each plan to identify the socially optimal transmission capacity (Virasjoki et al. 2020). Each QP problem instance takes a few seconds to solve to optimality with GAMS 35.1.0 using CPLEX 20.1.0.1 deployed on an Intel Core i7-8650U CPU@1.90 GHz quad-core processor and 16.0 GB of RAM. Looping through all 64 transmission plans takes approximately two hours for all values of D for a given value of H with the same hardware/software configuration.

4.2.3. Perfect competition

We summarise the numerical results for PC problem instances in Tables 13–15, where 'TC' refers to to which of the six lines is added/upgraded. Supplementary results about average nodal prices, average generation mixes, and average nodal net

Table 12. Transmission-line parameters for brownfield Western European case study.

Level and Line \ Attribute	$B_{j,\ell}$	$K^{\text{trn}}_{j,\ell}$	$C^{\text{trn}}_{j,\ell}$
$j1$ and $\ell1$	567	2,608	0
$j1$ and $\ell2$	1,404	2,372	0
$j1$ and $\ell3$	2,202	2,218	0
$j1$ and $\ell4$	845	3,867	0
$j1$ and $\ell5$	0	0	0
$j1$ and $\ell6$	0	0	0
$j2$ and $\ell1$	680	3,008	840,000
$j2$ and $\ell2$	1,727	2,772	840,000
$j2$ and $\ell3$	2,730	2,618	840,000
$j2$ and $\ell4$	1,027	4,267	840,000
$j2$ and $\ell5$	220	400	1,260,000
$j2$ and $\ell6$	138	400	1,600,000

Table 13. Numerical results for PC brownfield Western European case study with $H = 0$ (in M€ unless indicated).

Metric \ D	0	25	50	75	100
SW	2,059.31	1,912.55	1,767.15	1,622.49	1,477.84
CS	1,885.38	1,882.20	1,878.56	1,878.56	1,878.56
PS	164.15	168.27	170.47	170.47	170.47
MS	9.79	10.29	10.37	10.37	10.37
GR	0	0	0	0	0
DC	0	146.52	289.31	433.96	578.62
TP	0	1.68	2.94	2.94	2.94
EM (Mt)	5.88	5.86	5.79	5.79	5.79
GC (GW)	[0 0 0 0]	[0 0 0 0]	[0 0 0 0]	[0 0 0 0]	[0 0 0 0]
TC (–)	[0 0 0 0 0 0]	[1 1 0 0 0 0]	[1 1 0 0 1 0]	[1 1 0 0 1 0]	[1 1 0 0 1 0]

Table 14. Numerical results for PC brownfield Western European case study with $H = 0.50$ (in M€ unless indicated).

Metric \ *D*	0	25	50	75	100
SW	2,059.31	1,940.02	1,859.18	1,812.79	1,791.68
CS	1,885.38	1,733.16	1,653.80	1,587.89	1,497.06
PS	164.15	250.74	279.40	300.13	357.09
MS	9.79	12.78	15.84	20.72	28.38
GR	0	54.98	88.18	93.43	88.33
DC	0	109.97	176.35	186.86	176.66
TP	0	1.68	1.68	2.52	2.52
EM (Mt)	5.88	4.40	3.53	2.49	1.77
GC (GW)	[0 0 0 0]	[0 0 0 0]	[0 0 0 16.57]	[0 0 0 21.48]	[0 0 0 23.66]
TC (–)	[0 0 0 0 0 0]	[1 1 0 0 0 0]	[1 1 0 0 0 0]	[1 1 0 1 0 0]	[1 1 0 1 0 0]

Table 15. Numerical results for PC brownfield Western European case study with $H = 1$ (in M€ unless indicated).

Metric \ *D*	0	25	50	75	100
SW	2,059.31	1,947.36	1,880.24	1,845.81	1,819.97
CS	1,885.38	1,653.80	1,496.84	1,402.16	1,351.18
PS	164.15	270.40	357.09	409.08	430.37
MS	9.79	15.84	27.99	37.09	40.94
GR	0	88.18	89.78	88.04	90.23
DC	0	88.18	89.78	88.04	90.23
TP	0	1.68	1.68	2.52	2.52
EM (Mt)	5.88	3.53	1.80	1.17	0.90
GC (GW)	[0 0 0 0]	[0 0 0 16.57]	[0 0 0 22.99]	[0.44 0 0 26.05]	[6.88 0 0 27.39]
TC (–)	[0 0 0 0 0 0]	[1 1 0 0 0 0]	[1 1 0 0 0 0]	[1 1 0 1 0 0]	[1 1 0 1 0 0]

imports by D and H are given in Supplementary Appendix C. Starting with $H = 1$ in Table 15, we note that it is equivalent to CP and is the first-best solution as the social cost of damage from emissions is fully internalised. For $D = 0$, there is neither generation nor transmission investment, and node $n2$ is (nodes $n1$, $n3$, and $n4$ are) a net exporter (net importers) (Figure C-9). When $D = 25$ and $D = 50$, wind capacity is added at node $n4$ (the Netherlands). This is facilitated by expanding lines $\ell 1$ and $\ell 2$, which enables integration of VRE. For example, Germany goes from being a modest net importer at $D = 0$ to a heavy net importer at $D = 25$, while the Netherlands switches from being a net importer to a net exporter over this interval. Further increases to $D = 75$ and $D = 100$ lead to expansion of line $\ell 4$, thereby leveraging the complementarity between flexible plants and VRE while simultaneously diminishing emissions. In particular, CCGT capacity is adopted at node $n1$ (Germany) for $D = 75$ to complement additional wind capacity at node $n4$ (the Netherlands) as German coal and lignite operations are eliminated (Figure C-6).[15] A subsequent increase to $D = 100$ incentivises solely wind adoption at both nodes $n1$ and $n4$. Although the SW drops by about 12% as D increases from €0/t to €100/t, there is a change in its composition with a transfer from consumers to producers and higher average prices, viz., €32.05/MWh and €57.98/MWh for $D = 0$ and $D = 100$ (Figure C-3), respectively. Finally, CO_2 emissions decrease by nearly 85% as D goes from €0/t to €100/t.

By contrast, consider the situation with $H = 0$ in Table 13 in which node $n2$ is (nodes $n1$, $n3$, and $n4$ are) again a net exporter (net importers) for $D = 0$ (Figure C-7). Since the social cost of damage from CO_2 emissions cannot be internalised, the TSO attempts to mitigate it by altering the lines' capacities vis-à-vis the results with

$H = 1$. In effect, absent a carbon tax, consumption is not curbed and electricity prices do not increase, which means that generation investment is not triggered. Thus, going from $D = 0$ to $D = 25$ induces an expansion of lines $\ell 1$ and $\ell 2$ in order to increase exports from the existing nuclear capacity at node $n2$ (France) and to displace some coal and CCGT output at node $n4$ (the Netherlands). Once D increases from €25/t to €50/t, line $\ell 5$ is added to exploit the existing CCGT and gas-fired plants at nodes $n1$ (Germany), $n3$ (Belgium), and $n4$ (the Netherlands) (Figure C-4). Output from these relatively clean plants displaces coal-fired generation, mainly at node $n1$ (Germany). Further increases from $D = 50$ to $D = 100$ have no impact on investment and operational decisions because all of the existing generation capacity that is relatively clean and economically viable has been deployed. Due to a lack of pricing the externality, there is a decrease in SW of nearly 30% as D increases from €0/t to €100/t resulting from no incentive either to curb consumption or to invest in VRE, viz., the average prices are €32.05/MWh and €32.30/MWh for $D = 0$ and $D = 100$, respectively (Figure C-1). Overall, the impact of D on SW, EM, and other metrics indicates the limitations of using solely transmission planning to support decarbonisation without an adequate carbon price. Indeed, even a partial carbon price with $H = 0.50$ as in Table 14 improves key metrics and fully aligns the transmission plan with the first-best one in Table 15, albeit with less wind investment. In addressing RQ 1, we conclude that internalisation of the social cost of damage renders transmission planning more effective by ensuring an adequate price signal to reduce consumption and to stimulate generation investment and operations.

4.2.4. Cournot oligopoly

Under CO with $H = 0$ (Table 16), we first note that SW and CS are lower than those under PC, which is expected as average prices are higher, viz., €40.50/MWh instead of €32.05/MWh (Figure C-10). While PS is higher as anticipated, EM is also higher, which is somewhat counterintuitive. In fact, this outcome is related to the fringe firms' incentive to invest in CCGT plants at nodes $n2$ (France), $n3$ (Belgium), and $n4$ (the Netherlands) as a result of generation withholding à la Cournot by large firms to boost prices (Figure C-13). In effect, reduced output by nuclear plants at nodes $n2$ (France) and $n3$ (Belgium) means that all nodes are net importers except for node $n1$ (Germany) for $D = 0$ (Figure C-16). Due to the absence of VRE adoption, it is not warranted for the TSO to modify transmission capacity until $D = 100$, which

Table 16. Numerical results for CO brownfield Western European case study with $H = 0$ (in M€ unless indicated).

Metric \ D	0	25	50	75	100
SW	1,894.45	1,684.06	1,473.68	1,263.29	1,053.04
CS	1,642.61	1,642.61	1,642.61	1,642.61	1,648.73
PS	247.18	247.18	247.18	247.18	239.81
MS	4.67	4.67	4.67	4.67	3.90
GR	0	0	0	0	0
DC	0	210.39	421.78	631.16	838.14
TP	0	0	0	0	1.26
EM (Mt)	8.42	8.42	8.42	8.42	8.38
GC (GW)	[0 44.27 7.29 1.09]	[0 44.27 7.29 1.09]	[0 44.27 7.29 1.09]	[0 44.27 7.29 1.09]	[0 44.45 7.81 1.99]
TC (–)	[0 0 0 0 0 0]	[0 0 0 0 0 0]	[0 0 0 0 0 0]	[0 0 0 0 0 0]	[0 0 0 0 1 0]

prompts the addition of line $\ell 5$ to spur more CCGT investments at nodes $n3$ (Belgium) and $n4$ (the Netherlands). Consequently, coal output at node $n1$ (Germany) is modestly displaced as node $n3$ (Belgium) becomes a net exporter, but the overall impact on EM is minute because of the lack of internalisation of the social cost of damage from CO_2 emissions. More important, this absence of a price signal on emissions leads to a nearly 50% decrease in SW as D increases from €0/t to €100/t.

In a marked contrast, full internalisation of the social cost of damage from emissions with $H = 1$ in Table 17 enables wind capacity to be adopted at node $n4$ (the Netherlands) and limits new CCGT capacity at nodes $n2$–$n3$ (France and Belgium) even without any transmission expansion, e.g. when $D = 25$ (Figure C-15). This is because the internalisation of the social cost of damage from emissions gives the price signal to curb coal generation at node $n1$ (Germany). For example, the average price is €49.56/MWh for $D = 25$ when $H = 1$ instead of €40.50/MWh when $H = 0$ (Figure C-12). Because both consumption and coal generation are curbed, the existing transmission network is sufficient to integrate the additional wind capacity by reducing net imports by node $n4$ (the Netherlands) (Figure C-18), thereby enabling a sizeable reduction in EM. Once $D = 50$, an important milestone is reached with the elimination of coal generation altogether (Figure C-15).[16] Indeed, the average price of €57.86/MWh is high enough to engender further expansion of wind capacity at node $n4$ (the Netherlands), which is better balanced *via* the existing network topology by placing CCGT capacity adjacent to it at node $n1$ (Germany) instead of at nodes $n2$ and $n3$. Consequently, node $n4$ (the Netherlands) becomes a significant net exporter, while node $n1$ (Germany) increases its net imports. Only for $D = 75$ does the TSO intervene by reinforcing lines $\ell 3$ and $\ell 4$, which connect node $n4$ (the Netherlands) with nodes $n3$ (Belgium) and $n1$ (Germany), respectively. In conjunction with a reduction in consumption (as evidenced by an increase in the average price to €65.82/MWh) and elimination of lignite at node $n1$ (Germany), these expanded lines enable the additional wind output to displace CCGT capacity partly at adjacent nodes. As a result, net exports from node $n4$ (the Netherlands) increase, while nodes $n1$ (Germany) and $n3$ (Belgium) increase net imports. Once $D = 100$, another fundamental shift occurs in the generation mix as the average price of €71.39/MWh warrants significant adoption of wind capacity at nodes $n1$ (Germany) and $n2$ (France).

Table 17. Numerical results for CO brownfield Western European case study with $H = 1$ (in M€ unless indicated).

Metric \ D	0	25	50	75	100
SW	1,894.45	1,723.03	1,621.45	1,561.20	1,532.02
CS	1,642.61	1,440.03	1,268.39	1,117.51	1,032.96
PS	247.18	276.84	343.70	431.16	483.46
MS	4.67	6.16	9.35	14.21	17.27
GR	0	142.15	196.92	220.80	144.89
DC	0	142.15	196.92	220.80	144.89
TP	0	0	0	1.68	1.68
EM (Mt)	8.42	5.69	3.94	2.94	1.45
GC (GW)	[0 44.27 7.29 1.09]	[0 39.69 6.72 20.00]	[4.05 35.76 5.84 24.55]	[3.69 31.08 4.55 28.03]	[18.92 85.78 3.18 28.84]
TC (–)	[0 0 0 0 0 0]	[0 0 0 0 0 0]	[0 0 0 0 0 0]	[0 0 1 1 0 0]	[0 0 1 1 0 0]

In spite of increased wind adoption, the system is less reliant on CCGT output with increased net exports from node $n2$ (France). Likewise, no changes to the transmission capacity are necessary in this final increment to D since reduced consumption enables balancing of the system. As in the PC case with $H = 1$, CO_2 emissions are reduced by over 80% in going from $D = 0$ to $D = 100$. Moreover, in spite of this substantial decarbonisation, overall SW decreases by only 15% as D increases from €0/t to €100/t, cf. 50% for $H = 0$. Thus, in addressing RQ 2, we observe that full internalisation of D is optimal even under imperfect competition. Finally, a partial carbon price with $H = 0.50$ (Table 18) nearly results in the optimal network topology apart from $D = 50$, which leads to an insufficient incentive for elimination of coal at node $n1$ (Germany) and the need to add line $\ell 3$ instead.

In contrast to the PC cases, increasing H from zero under CO actually increases transmission expansion. This is because insufficient carbon pricing under PC leads to overconsumption and no incentive to adopt any generation capacity, which the TSO mitigates by 'rearranging the deck chairs' as D increases *ceteris paribus*, i.e. adding transmission capacity to marshal existing CCGT capacity in a vain attempt to limit coal generation. Once the social cost of damage from CO_2 emissions is internalised with a high H, the TSO adds a similar amount of transmission capacity but with a different topology in order to ensure that the adopted wind capacity is complemented by enough CCGT capacity. However, under CO, modestly high prices and a lack of carbon pricing for $H = 0$ trigger investment in the 'wrong' generation technology, such as CCGT instead of wind. The TSO has no leverage to incentivise investment in wind and can only add a new line to displace coal generation by CCGT output as D increases *ceteris paribus*. A sufficient increase in H alleviates this distortion and bolsters the need to expand transmission capacity because higher prices induce the adoption of wind capacity, which requires network reinforcement for balancing output. Thus, internalisation of the social cost of damage from CO_2 emissions has distinct impacts on transmission planning depending on the exercise of market power, viz., whether the TSO needs to alleviate either overconsumption and a lack of investment in VRE (under PC) or an excessive adoption of CCGT (under CO), which addresses RQs 1–2. Moreover, we gain insights about the impact of market structure on transmission expansion. In the case study, the presence of fringe firms with the propensity to invest in CCGT dilutes (intensifies) the concerns about market power (CO_2

Table 18. Numerical results for CO brownfield Western European case study with $H = 0.50$ (in M€ unless indicated).

Metric \ D	0	25	50	75	100
SW	1,894.45	1,713.00	1,580.98	1,493.41	1,425.27
CS	1,642.61	1,542.17	1,440.07	1,349.51	1,268.61
PS	247.18	252.74	276.93	308.72	343.71
MS	4.67	4.24	6.57	8.02	10.39
GR	0	86.15	141.75	171.16	195.76
DC	0	172.30	283.49	342.33	391.51
TP	0	0	0.84	1.68	1.68
EM (Mt)	8.42	6.89	5.67	4.56	2.63
GC (GW)	[0 44.27 7.29 1.09]	[0 41.40 6.98 9.88]	[0 39.65 6.51 20.54]	[3.00 38.37 6.05 24.27]	[3.82 35.73 5.54 25.73]
TC (–)	[0 0 0 0 0 0]	[0 0 0 0 0 0]	[0 0 1 0 0 0]	[0 0 1 1 0 0]	[0 0 1 1 0 0]

emissions). Hence, in contrast to the results from the illustrative greenfield example, increasing the carbon price monotonically enhances social welfare while enabling spatial balancing *via* transmission expansion.

5. Discussion and conclusions

The decarbonisation of the power sector envisages an unprecedented investment in VRE capacity with sufficient transmission capacity to mitigate spatio-temporal variability. However, this is a challenging objective to achieve in a deregulated industry with power companies that may exert market power. With a few notable exceptions, the extant literature uses either detailed problem instances without directly accounting for the cost of damage from emissions or stylised models based on environmental economics that ignore the spatio-temporal texture of realistic power systems.

Given the research gap, we specifically tackle RQs 1–2 *via* an illustrative greenfield example and a brownfield Western European case study. We use a bi-level approach to compare PC and CO settings in analysing sustainable transmission expansion. Concerning RQ 1, under PC, a lack of curb on consumption leads to lower transmission capacities in the illustrative example, but a carbon price internalises the damage cost and increases transmission capacity to support VRE adoption with a monotonic increase in welfare. The finding is similar for the case study, albeit the network topology is more affected than the transmission capacity. Absent a carbon price, the TSO changes the network topology in a futile attempt to squeeze more output from relatively clean plants, viz., nuclear and CCGT, to displace coal production. By contrast, the answer to RQ 2 varies between the illustrative example and the case study. Intuitively, full carbon pricing under CO in the illustrative example excessively curbs consumption and reduces welfare vis-à-vis partial carbon pricing, which cannot be mitigated by a countervailing transmission plan. In the case study, however, the combination of high prices due to Cournot firms' withholding output and investment in CCGT capacity by fringe firms mitigates the concern about market power but bolsters the cost of damage from CO_2 emissions. The contrast between PC and CO is that absent a carbon price, the TSO under CO has even less scope for intervention as high prices engendered by market power incentivise investment in the 'wrong' types of power plants, i.e. CCGT, which are flexible enough to obviate the need for expanded transmission capacity. In effect, full carbon pricing under CO drives both curbs in consumption and investment in VRE, which the TSO complements by adding transmission capacity. Hence, social welfare monotonically increases in the carbon tax levied on industry.

While our model examines transmission planning under economic and environmental distortions in both greenfield and brownfield settings, it abstracts away from explicit handling of uncertainty in demand and VRE output in order to keep problem instances computationally tractable. Likewise, it also takes CO_2 pricing as exogenous, and the solution approach based on MPPDC does not scale beyond the greenfield problem instances. Thus, future work in this area could expand along three axes. First, a stochastic model could be devised with scenarios for VRE availability and demand realisations. Such a framework would also open up the possibility to conduct risk management. Second, in a different direction, we could focus on endogenous carbon pricing (Dimanchev and Knittel 2023) at the upper level in anticipation of generation investment plus operations at the lower level. Finally, a methodological line of investigation would be improved numerical-resolution methods based on either decomposition (Andrade et al. 2022) or parametric programming (Bylling et al. 2020) for the MIQCQP problem instances with the Western European test network.

Notes

1. https://ec.europa.eu/info/strategy/priorities-2019-2024/european-green-deal_en.
2. This modelling feature is intended to avoid unrealistic outcomes in which intermittent output from substantial VRE capacity additions would be balanced by idle flexible capacity. In fact, high VRE penetration may depress prices to the extent that flexible capacity would not be able to cover its fixed O&M costs from operating profits. In reality, power plants are mothballed in the event that their fixed O&M costs cannot be covered by market revenues.
3. VRE units have zero operating costs and emission rates.
4. https://news.stanford.edu/2021/06/07/professors-explain-social-cost-carbon/.
5. We assume that PHS capacities are given and cannot be altered, which reflects the paucity of geographically amenable sites for storage.
6. Note that constraints (1d)–(1e) are linearised from the original nonlinear versions $f_{j,\ell,m,t} = x_{j,\ell} B_{j,\ell}(v_{n_\ell^+,m,t} - v_{n_\ell^-,m,t}), \forall \ell, m, t, j \in \mathcal{J}_\ell$ and $-T_t K_{j,\ell}^{\text{trn}} \leq T_t f_{j,\ell,m,t} \leq T_t K_{j,\ell}^{\text{trn}}, \forall \ell, m, t, j \in \mathcal{J}_\ell$, respectively. Through the use of $x_{j,\ell}$ and M^{trn}, (1d)–(1e) disjunctively linearise the latter two equations by restricting $f_{j,\ell,m,t}$ to be equal to $B_{j,\ell}(v_{n_\ell^+,m,t} - v_{n_\ell^-,m,t})$ only if $x_{j,\ell} = 1$. Otherwise, if $x_{j,\ell} = 0$, then $f_{j,\ell,m,t}$ is forced to zero.
7. Given $x_{j,\ell}$, the lower level comprises (i) the profit-maximisation problems of firms, $i \in \mathcal{I}$, and (ii) the ISO's surplus-maximisation problem. This equilibrium problem that reflects the Nash-Cournot game over a given network at the lower level may be rendered as a single-agent QP (Hashimoto 1985).
8. For sake of brevity, Ω^{DV} includes the auxiliary variable, $\hat{\mu}_{j,\ell,m,t}$, which is introduced in the MIQCQP.
9. https://www.eia.gov/tools/faqs/faq.php?id=73&t=11.
10. https://www.eia.gov/analysis/studies/powerplants/capitalcost/pdf/capital_cost_AEO2020.pdf.
11. It should be noted that the parameters $\underline{G}_{m,n,t,u}$ and $\overline{G}_{m,n,t,u}$ are 0 and 1 for the other two technologies, i.e. they are fully flexible subject to their installed capacities and ramp rates.
12. It should be noted that the minimum-availability parameter, $\underline{G}_{m,n,t,u}$, is 0 for the non-VRE technologies. As for the maximum-availability parameter, $\overline{G}_{m,n,t,u}$, it ranges between 0.80 and 0.89 for thermal units ($u1$–$u6$) but is derated to 0.30 for hydro units ($u7$) to reflect their dependency on exogenous inflows. Thus, non-VRE technologies are fully flexible between $\underline{G}_{m,n,t,u}$ and $\overline{G}_{m,n,t,u}$ subject to their installed capacities and ramp rates.
13. https://www.eia.gov/tools/faqs/faq.php?id=73&t=11.
14. https://www.eia.gov/analysis/studies/powerplants/capitalcost/pdf/capital_cost_AEO2020.pdf.
15. For example, lignite's effective operating cost becomes $C_u^{\text{opr}} + F_u \times H \times D =$ €11.2/MWh+0.94 t/MWh x 1 x €75/t = €81.7/MWh.
16. For example, coal's effective operating cost becomes $C_u^{\text{opr}} + F_u \times H \times D =$ €27.4/MWh+0.83 t/MWh x 1 x €50/t = €68.9/MWh.

Disclosure statement

Afzal Siddiqui reports a relationship with the Research Institute of Industrial Economics that includes: consulting or advisory.

Funding

Siddiqui's work has been funded by the Swedish Energy Agency (Energimyndigheten) under grant numbers 49259-1 [STRING: Storage, Transmission, and Renewable Interactions in the Nordic Grid] and P2023-00433 [SCORES: Sector Coupling and Operational Research for Environmental Sustainability]. We have benefited from feedback received at the 2021 INFORMS Annual Meeting, the 2021 Trans-Atlantic Cooperation on Energy Market Modeling, and the 2022 EURO Conference as well as a seminar at HEC Montréal. We are grateful to the handling editor and an anonymous reviewer for providing detailed feedback. All remaining errors are the authors' own.

ORCID

Afzal S. Siddiqui http://orcid.org/0000-0003-1841-1310
Makoto Tanaka http://orcid.org/0000-0002-8606-865X

Data availability statement

Data used in the greenfield illustrative example are synthetically generated as desribed in Section 4.1.1. Meanwhile, the brownfield Western European case study in Section 4.2.1 uses the dataset from Virasjoki et al. (2020), which is a publicly available journal article.

References

Andrade T, Belyak N, Eberhard A, Hamacher S, Oliveira F. 2022. The p-Lagrangian relaxation for separable nonconvex MIQCQP problems. J Glob Optim. 84(1):43–76. https://doi.org/10.1007/s10898-022-01138-y

Arora V, Daniels D, Mead I, Tarver R. 2018. EMF32 results from NEMS: revenue recycling. Clim Change Econ. 09(01):1840014. https://doi.org/10.1142/s2010007818400146

Baringo L, Conejo AJ. 2012. Transmission and wind power investment. IEEE Trans Power Syst. 27(2):885–893. https://doi.org/10.1109/TPWRS.2011.2170441

Barnett AH. 1980. The Pigouvian tax rule under monopoly. Amer Econ Rev. 70(5):1037–1041.

Belyak N, Gabriel SA, Khabarov N, Oliveira F. 2024. Renewable energy expansion under taxes and subsidies: a transmission operator's perspective. J Cleaner Prod. 451:141955. https://doi.org/10.1016/j.jclepro.2024.141955

Bylling HC, Gabriel SA, Boomsma TK. 2020. A parametric programming approach to bilevel optimisation with lower-level variables in the upper level. J Oper Res Soc. 71(5):846–865. https://doi.org/10.1080/01605682.2019.1590132

Cambini R, Riccardi R. 2024. Optimality conditions for differentiable linearly constrained pseudoconvex programs. Decisions Econ Finan. 47(2):497–512. https://doi.org/10.1007/s10203-024-00454-0

Chen Y, Siddiqui AS, Tanaka M. 2020. Analysis of environmental policy in the power sector. Springer.

Dimanchev E, Knittel CR. 2023. Designing climate policy mixes: analytical and energy system modeling approaches. Ener Econ. 122:106697. https://doi.org/10.1016/j.eneco.2023.106697

Egerer J. 2016. Open source electricity model for Germany. DIW https://www.diw.de/documents/publikationen/73/diw_01.c.528927.de/diw_datadoc_2016-083.pdf

Gabriel SA, Conejo AJ, Fuller JD, Hobbs BF, Ruiz C. 2013. Complementarity modeling in energy markets. Springer.
García-Cerezo Á, Siddiqui AS, Boomsma TK, García-Bertrand R, Baringo L. 2025. Strategic investment in electricity markets: robust optimization versus stochastic programming. Eur J Oper Res. forthcoming. https://doi.org/10.1016/j.ejor.2025.08.009
Garver LL. 1970. Transmission network estimation using linear programming. IEEE Trans Power Apparatus Syst. PAS-89 (7):1688–1697. https://doi.org/10.1109/TPAS.1970.292825
Hashimoto H. 1985. A spatial Nash equilibrium model. In: Harker P, editor, Spatial price equilibrium: advances in theory, computation and application. Springer. p. 20–40. https://doi.org/10.1007/978-3-642-46548-2_2
Hassanzadeh Moghimi F, Boomsma TK, Siddiqui AS. 2024. Transmission planning in an imperfectly competitive power sector with environmental externalities. Ener Econ. 134: 107610. https://doi.org/10.1016/j.eneco.2024.107610
Hobbs BF. 1995. Optimization methods for electric utility resource planning. Eur J Oper Res. 83(1):1–20. https://doi.org/10.1016/0377-2217(94)00190-N
Hobbs BF. 2001. Linear complementarity models of Nash-Cournot competition in bilateral and POOLCO power markets. IEEE Trans Power Syst. 16(2):194–202. https://doi.org/10.1109/59.918286
Hobbs BF. 2012. Transmission planning and pricing for renewables: lessons from elsewhere. IEEE Power and Energy Society General Meeting. https://doi.org/10.1109/PESGM.2012.6344744
Huppmann D, Egerer J. 2015. National-strategic investment in European power transmission capacity. Eur J Oper Res. 247(1):191–203. https://doi.org/10.1016/j.ejor.2015.05.056
Labriet M, Loulou R. 2003. Coupling climate damages and GHG abatement costs in a linear programming framework. Env Mod & Ass. 8(3):261–274. https://doi.org/10.1023/A:1025503525777
Lau J, Hobbs BF. 2021. Electricity transmission system research and development: economic analysis and planning tools, U.S. Department of Energy. https://www.energy.gov/sites/default/files/2021-05/Economic%20Analysis%20and%20Planning%20Lau%20Hobbs2.pdf.
Mahmoud HA, Sharaf M, El-Meligy MA. 2024. An adaptive robust optimization model for transmission expansion planning considering uncertain intervals. Int J Elec Power & Ener Syst. 157:109821. https://doi.org/10.1016/j.ijepes.2024.109821
Mariscal F, Reyes T, Sauma E. 2020. Valuing flexibility in transmission expansion planning from the perspective of a social planner: a methodology and an application to the Chilean power system. The Eng Econ. 65(4):288–320. https://doi.org/10.1080/0013791X.2020.1712509
Maurovich-Horvat L, Boomsma TK, Siddiqui AS. 2015. Transmission and wind investment in a deregulated electricity industry. IEEE Trans Power Syst. 30(3):1633–1643. https://doi.org/10.1109/TPWRS.2014.2367107
Neuhoff K et al. 2005. Network-constrained cournot models of liberalized electricity markets: the devil is in the details. Ener Econ. 27(3):495–525. https://doi.org/10.1016/j.eneco.2004.12.001
Requate T. 2006. Environmental policy under imperfect competition. In: Tietenberg T, Folmer H, editors. The international yearbook of environmental and resource economics 2006/2007: a survey of current issues. Edward Elgar Publishing. p. 120–187.
Rintamäki T, Oliveira F, Siddiqui AS, Salo A. 2024. Achieving emission-reduction goals: multiperiod power-system expansion under short-term operational uncertainty. IEEE Trans Power Syst. 39(1):119–131. https://doi.org/10.1109/TPWRS.2023.3244668
Rodríguez-Sarasty JA, Debia S, Pineau P-O. 2021. Deep decarbonization in Northeastern North America: the value of electricity market integration and hydropower. Ener Pol. 152: 112210. https://doi.org/10.1016/j.enpol.2021.112210
Sauma EE, Oren SS. 2006. Proactive planning and valuation of transmission investments in restructured electricity markets. J Regul Econ. 30(3):261–290. https://doi.org/10.1007/s11149-006-9003-y

Siddiqui AS, Tanaka M, Chen Y. 2019. Sustainable transmission planning in imperfectly competitive electricity industries: balancing economic and environmental outcomes. Eur J Oper Res. 275(1):208–223. https://doi.org/10.1016/j.ejor.2018.11.032

Skoulidas CC, Vournas CD, Papavassilopoulos GP. 2010. An adaptive learning game model for interacting electric power markets. INFOR: inf Syst & Oper Res. 48(4):261–266. https://doi.org/10.3138/infor.48.4.261

Sun Y, Xu Q, Hobbs BF. 2025. Can proactive electric transmission planning cost-effectively mitigate carbon emissions? A Western North America Case study. Ener Econ. 148:108591. https://doi.org/10.1016/j.eneco.2025.108591

Tanaka M, Conejo AJ, Siddiqui AS. 2022. Economics of power systems. Springer.

Virasjoki V, Siddiqui AS, Oliveira F, Salo A. 2020. Utility-scale energy storage in an imperfectly competitive power sector. Ener Econ. 88:104716. https://doi.org/10.1016/j.eneco.2020.104716

Wilson R. 2002. Architecture of power markets. Econometrica. 70(4):1299–1340. https://doi.org/10.1111/1468-0262.00334

Yin X, Chen H, Liang Z, Zhu Y. 2023. A flexibility-oriented robust transmission expansion planning approach under high renewable energy resource penetration. Appl Energy. 351:121786. https://doi.org/10.1016/j.apenergy.2023.121786

Zeng X et al. 2024. Highly-efficient single-level robust transmission expansion planning approach applicable to large-scale renewable energy integration. Sust Ener Grids Netw. 39:101486. https://doi.org/10.1016/j.segan.2024.101486